Weierstraß-Institut
für Angewandte Analysis und Stochastik

im Forschungsverbund Berlin e.V.

Preprint ISSN 0946 – 8633

Random Walk on Fixed Spheres for Laplace and Lamé equations

K. K. Sabelfeld[1,2], I. A. Shalimova[2], and A. I. Levykin[2]

[1] Weierstrass Institute for Applied Analysis and Stochastics,
Mohrenstrase 39. D – 10117 Berlin, Germany;
E-Mail: sabelfel@wias-berlin.de,

[2] Institute of Comp. Mathematics and Mathem. Geophysics,
Russian Acad. Sci., Lavrentieva str., 6, 630090 Novosibirsk, Russia

No. 1106
Berlin 2006

1991 *Mathematics Subject Classification.* 65C05, 65C20, 65Z05.

Key words and phrases. Poisson integral formula, Random Walk on Fixed Spheres, Lamé equation, Successive Over Relaxation Method, Divergent Neumann series, Discrete Random Walks .

This work is supported partly by DFG Grants 436 RUS 17/24/05 and 436 RUS 17/27/05, and NATO Collaborative Linkage Grant CLG N 981426.

Edited by
Weierstraß-Institut für Angewandte Analysis und Stochastik (WIAS)
Mohrenstraße 39
10117 Berlin
Germany

Fax: + 49 30 2044975
E-Mail: preprint@wias-berlin.de
World Wide Web: http://www.wias-berlin.de/

Abstract

The Random Walk on Fixed Spheres (RWFS) introduced in our paper [25], and further developed in [26], is presented in details for Laplace and Lamé equations governing static elasticity problems. The approach is based on the Poisson type integral formulae written for each disc of a domain consisting of a family of overlapping discs. The original differential boundary value problem is equivalently reformulated in the form of a system of integral equations defined on the intersection surfaces (arches, in 2D, and caps, if generalized to 3D spheres). To solve the obtained system of integral equations, a Random Walk procedure is constructed where the random walks are living on the intersecting surfaces. Since the spheres are fixed, it is convenient to construct also discrete random walk methods for solving the system of linear equations approximating the system of integral equations. We develop here two classes of special Monte Carlo iterative methods for solving these systems of linear algebraic equations which are constructed as a kind of randomized versions of the Chebyshev iteration method and Successive Over Relaxation (SOR) method. It is found that in this class of randomized SOR methods, the Gauss-Seidel method has a minimal variance. In [25] we have concluded that in the case of classical potential theory, the Random Walk on Fixed Spheres considerably improves the convergence rate of the standard Random Walk on Spheres method. More interesting, we succeeded there to extend the algorithm to the system of Lamé equations which cannot be solved by the conventional Random Walk on Spheres method. We present here a series of numerical experiments for 2D domains consisting of 5, 10, and 17 discs, and analyze the dependence of the variance on the number of discs and elastic constants. Further generalizations to Neumann and Dirichlet-Neumann boundary conditions are possible, see [23].

1. Introduction

There are two main classes of stochastic numerical methods for solving PDEs:
(1) methods based on probabilistic representations of solutions in the form of expectations over diffusion stochastic processes (e.g., see [4], [15]), (2) methods based on Markov chain simulation technique for solving integral equations; here the crucial point is the reformulation of the original boundary value problem in the form of integral equation [5], [6], [22].

The probabilistic representations are possible however only for scalar elliptic and parabolic equations, e.g., see [4]. Even in this case, considerable difficulties arise when approximating the random process near the boundary: one should take care that in each step, the simulated diffusion process is inside the domain. This implies a rapid diminishing of the integration step when approaching the boundary, which in turn rapidly increases the computational cost [15]. Exterior boundary value problems are hard or better to say impossible to solve by a numerical simulation of diffusion processes in unbounded regions.

The methods based on integral equation reformulation are much more flexible. Generally, any boundary value problem transformed into an integral form can be solved by a Markov chain simulation technique. It should be noted however that the Monte Carlo methods for solving integral equations are traditionally applied to integral equations $v = Kv + f$ with substochastic kernels when $\|K\| < 1$. The method was first developed for solving linear radiative transfer equations, and the famous Neumann-Ulam scheme works under the condition that the Neumann series converges.

The first Monte Carlo method for integral equations with divergent Neumann series was suggested by K. Sabelfeld in [21], and further developed in [22], [29]. The method is based on a conformal transformation of the spectral parameter. In this approach the variance analysis is much more difficult than in the Neumann-Ulam method. Nevertheless, it opens new interesting possibilities of applications. For example, the Random Walk on Boundary methods were constructed first for Dirichlet problem in [21], and then generalized in [29] to all classical interior and exterior boundary value problems of the electrostatic, heat and elastic potential theory. Note that in this case, there are no difficulties with the boundary conditions and exterior problems. As to the disadvantages of this class of methods, the variance of the method may be large for highly non-convex domains. However special versions of this methods for such domains can be developed, in particular, based on a discretization of the boundary integral equations, or using branching Random Walk on Boundary process [24].

In this paper, we deal with a new class of Markov chain simulation technique for systems of elliptic equations. The method differs from the conventional Random Walk on Spheres method in the following points: (1) The spheres are not randomly chosen, instead, they are deterministically fixed so that the original domain is well approximated by this set of spheres; (2) The randomized evaluation of the solution via the iterations of integrals follows not the Neumann-Ulam scheme, but a different iterative method, e.g., the Chebyshev iterations, or the Successive Over Relaxation (SOR) method; (3) Since the phase space is fixed, one may introduce its discretization, and construct discrete Random Walks.

It should be noted that one can think of different combinations of (1)-(3). For example, the choice (1) means that the phase space is fixed, and the Random Walk is constructed on the set of fixed spheres; (1) and (2) means that the relevant iteration procedure is constructed directly for integral operators, and finally, with (1) - (3) we turn to the discrete Random Walk method organized according to the relevant iterative procedure.

Thus the idea of the method is that the original boundary value problem is reformulated in an integral form derived from the spherical mean value relations for fixed overlapped discs (see also [1], [3]). The basic approach is described in our book [27]. In [28], we have extended this approach by using the Poisson integral formula for overlapping spheres, and considered the relevant system of integral equations. The kernel of the Poisson integral formula was the generating transition probability density function of the Markov chain. The iterative procedure was actually a randomized method of simple iterations. Generally, this iterative procedure diverges in the case of Lamé equation. Therefore, we have introduced different iteration methods, in particular, an iterative procedure with random parameters, which coincides in the deterministic limit with Chebyshev's method, and a randomized SOR. A general discrete random walk scheme can be constructed through a discrete approximation of our system of integral equations. Surprisingly, this not only has complicated the method, but in contrary, we have obtained a convenient fast convergent method with a finite variance. Note that extensions from discs to ellipses can be readily done by using the relevant Poisson formula for ellipses, e.g., see [20]. Generalization to 3D case is also quite simple, since the Poisson kernel is explicitly known.

The paper is organized as follows. In Section 2 we present the main idea of the method for a simple case of 2D Laplace equation, and study the main properties of the generating integral equation. Section 3 deals with the system of elliptic equations, the so-called Lamé equation governing the elastic deformations of 2D bodies. In Section 4 we present iteration methods we use to construct Random Walk algorithms. For this purpose we use an iteration method with randomly chosen parameters, introduced by Vorobiev (e.g., see [13], [31]) and the SOR method which is particularly efficient for a special class of domains which we call DS_2-domains. Detailed description of Random Walk algorithms are given in Section 5, and numerical simulations are presented in Section 6.

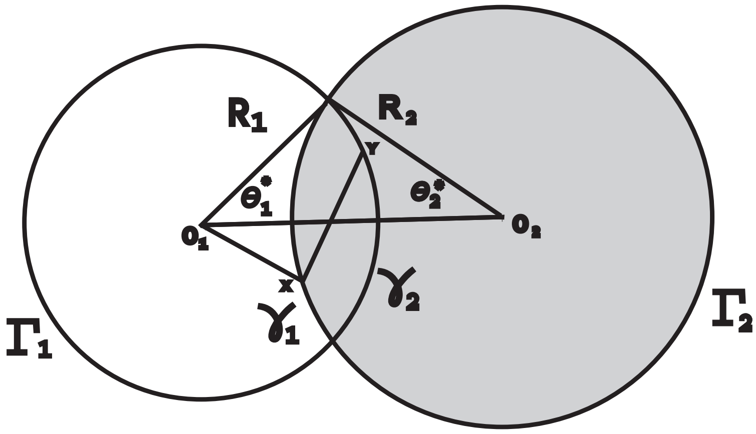

Figure 1: Two overlapping discs illustrating the main notations.

2. 2D Laplace equation

To explain the main idea of the method, we present here the case of two-dimensional Dirichlet problem for the Laplace equation. It should be noted that even in this simple case where the conventional Random Walk on Spheres works as well, the new method converges much faster, and the accuracy achieved is considerably higher.

2.1 Integral formulation of the Dirichlet problem

Let us consider the boundary value problem

$$\Delta u(x) = 0, \quad x \in D, \quad u(y) = \varphi, \quad y \in \Gamma = \partial D, \tag{2.1}$$

where the domain D consists of two overlapping discs $K(x_0^{(1)}, R_1)$ and $K(x_0^{(2)}, R_2)$ centered at $O_1 = x_0^{(1)}$ and $O_2 = x_0^{(2)}$ (see Figure 1):

$$D = K(x_0^{(1)}, R_1) \cup K(x_0^{(2)}, R_2); \quad K(x_0^{(1)}, R_1) \cap K(x_0^{(2)}, R_2) \neq \emptyset\ . \tag{2.2}$$

We denote by γ_2 the part of the circle $S(x_0^{(1)}, R_1) = \partial K(x_0^{(1)}, R_1)$ which belongs to the second disc while Γ_1 is the part of the circle $S(x_0^{(1)}, R_1)$ not belonging to the second disc; analogously γ_2 and Γ_2 are defined. So the boundary of the domain D consists of Γ_1 and Γ_2, and $\gamma_1 \cup \gamma_2$ is the phase space of the integral equation to be constructed.

The regular solution to the harmonic equation satisfies the spherical mean value relation in each of the two discs:

$$u(x) \quad = \quad \frac{R^2 - r^2}{2\pi R} \int\limits_{S(O,R)} \frac{u(y)dS_y}{|x-y|^2}\ . \tag{2.3}$$

Here $R = R_1$ in the first, and $R = R_2$ in the second disc, and the same for $r = |x - x_0^{(i)}|$, the distance from $x \in \gamma_i$ to the circle's center $O = O_i$, $i = 1, 2$.

It is not difficult to find out that the function

$$p(y;x) = \frac{R_1^2 - |x - x_0^{(1)}|^2}{2\pi R_1} \cdot \frac{1}{|x-y|^2} \tag{2.4}$$

is a probability density function of the variable $y \in S(x_0^{(1)}, R_1)$, for all $x \in K(x_0^{(1)}, R_1)$. This immediately follows from the representation of the solution $u = 1$ to the Dirichlet problem for the Laplace equation $\Delta u(x) = 0$, $u(y) = 1$ through the Poisson integral. From the probabilistic representation of the Dirichlet boundary value problem considered, the density $p(y;x)$ coincides with the probability density function (pdf) of the first passage on $S(x_0^{(1)}, R_1)$ of a Wiener process starting at $x \in K(x_0^{(1)}, R_1)$. Simple simulation of the transition according to (2.4) is given in [9].

It is possible to find explicitly the distribution function $P(x \to y \in \gamma)$ - the probability for a particle starting at $x \in S(x_0, R)$, with $r = |x - x_0|$, to reach an arc $\gamma \in S(x_0, R)$ defined by the limit angles α_1 and α_2, say, $\alpha_1 < \alpha_2$, since (e.g., see [7]):

$$\begin{aligned} P(x \to y \in \gamma) &= \frac{R^2 - r^2}{2\pi R} \int\limits_{\gamma} \frac{dS_y}{|x-y|^2} = \frac{1}{\pi} arctg \left\{ \frac{R+r}{R-r} tg \frac{\alpha}{2} \right\} \Bigg|_{\alpha_1}^{\alpha_2} \\ &= \frac{1}{\pi} arctg \left\{ \frac{R+r}{R-r} tg \frac{\alpha_2}{2} \right\} - \frac{1}{\pi} arctg \left\{ \frac{R+r}{R-r} tg \frac{\alpha_1}{2} \right\} . \end{aligned} \tag{2.5}$$

Let us now write down the Poisson formulae for both discs in the form

$$\begin{aligned} u(x) &= \frac{R_1^2 - |x - x_0^{(1)}|^2}{2\pi R_1} \int\limits_{S(x_0^{(1)}, R_1)} \frac{u(y)}{|x-y|^2} dS_y , \quad x \in \gamma_1 , \\ u(y) &= \frac{R_2^2 - |y - x_0^{(2)}|^2}{2\pi R_2} \int\limits_{S(x_0^{(2)}, R_2)} \frac{u(x')}{|y-x'|^2} dS_{x'} , \quad y \in \gamma_2 . \end{aligned} \tag{2.6}$$

We can give different equivalent formulations of the boundary value problem starting from these Poisson formulae. First, let us derive a scalar Fredholm linear integral equation of the second kind for the solution $u(x)$. To this end, we define the kernel $K(x,y)$, $x, y \in \gamma_1 \cup \gamma_2$ as follows. For $x \in \gamma_1$:

$$K(x,y) = \begin{cases} 0, & y \in \gamma_1 \\ k_{11}(x,y) = \frac{R_1^2 - |x - x_0^{(1)}|^2}{2\pi R_1} \frac{1}{|x-y|^2}, & y \in \gamma_2 \end{cases} ,$$

and for $x \in \gamma_2$:

$$K(x,y) = \begin{cases} 0, & y \in \gamma_2 \\ k_{22}(x,y) = \frac{R_2^2 - |x - x_0^{(2)}|^2}{2\pi R_2} \frac{1}{|x-y|^2}, & y \in \gamma_1 \end{cases} .$$

Using this notation we can rewrite the formulae (2.6) as follows:

$$u(x) = \int\limits_{\gamma_1 \cup \gamma_2} K(x,y) \, u(y) \, dS(y) + f(x) \tag{2.7}$$

where

$$\begin{aligned} f(x) &= \frac{R_1^2 - |x - x_0^{(1)}|^2}{2\pi R_1} \int\limits_{\Gamma_1} \frac{\varphi(y)}{|x-y|^2} dS_y , \quad \text{for } x \in \gamma_1, \\ f(x) &= \frac{R_2^2 - |x - x_0^{(2)}|^2}{2\pi R_2} \int\limits_{\Gamma_2} \frac{\varphi(y)}{|x-y|^2} dS_y , \quad \text{for } x \in \gamma_2 . \end{aligned} \tag{2.8}$$

Note that this equation is not symmetric, but we can show that it can be symmetrized. Indeed, let us introduce a new function by

$$w(x) = u(x)\sqrt{\frac{R_i}{R_i^2 - |x - x_0^{(i)}|^2}}, \qquad x \in \gamma_i, \quad i = 1,2\ .$$

Then we get the following equation

$$w(x) = \int\limits_{\gamma_1 \cup \gamma_2} \tilde{K}(x,y)\, w(y)\, dS(y) + f(x)\ , \tag{2.9}$$

where for $x \in \gamma_1$

$$\tilde{K}(x,y) = \begin{cases} 0, & y \in \gamma_1 \\ \frac{1}{2\pi}\frac{1}{|x-y|^2}\sqrt{\frac{R_1^2 - |x-x_0^{(1)}|^2}{R_1}}\sqrt{\frac{R_2^2 - |y-x_0^{(2)}|^2}{R_2}}, & y \in \gamma_2\ , \end{cases}$$

and for $x \in \gamma_2$:

$$\tilde{K}(x,y) = \begin{cases} 0, & y \in \gamma_2 \\ \frac{1}{2\pi}\frac{1}{|x-y|^2}\sqrt{\frac{R_1^2 - |y-x_0^{(1)}|^2}{R_1}}\sqrt{\frac{R_2^2 - |x-x_0^{(2)}|^2}{R_2}}, & y \in \gamma_1\ . \end{cases}$$

Thus we come to the integral equation with the symmetric kernel $\tilde{K}(x,y)$

$$w(x) = \int\limits_{\gamma_1 \cup \gamma_2} \tilde{K}(x,y)\, w(y)\, dS(y) + f(x)\ . \tag{2.10}$$

This implies that the eigenvalues of the integral operator defined by the kernel $K(x,y)$ in (2.7) are all real, moreover, we will give below the explicit expression for the principal eigenvalue of this integral operator.

As mentioned above, it is possible to give a different equivalent integral equation formulation of the problem under study.

Let us introduce the notation: $v_1(x) = u(x)$ for $x \in \gamma_1$, and $v_2(x) = u(x)$ for $x \in \gamma_2$. Then, (2.7) reads

$$v_1(x) = \int\limits_{\gamma_2} p(y;x) v_2(y)\, dS_y + f_1(x), \quad v_2(x) = \int\limits_{\gamma_1} p(x';x) v_1(x')\, dS_{x'} + f_2(x), \tag{2.11}$$

where

$$f_1(x) = \int\limits_{\Gamma_1} p(y;x)\varphi(y)\, dS_y, \quad f_2(x) = \int\limits_{\Gamma_2} p(x';x)\varphi(x')\, dS_{x'}\ . \tag{2.12}$$

It is convenient to rewrite the system (2.11) in the matrix form:

$$\mathbf{v} = \mathbf{G}\mathbf{v} + \mathbf{F} \tag{2.13}$$

where $\mathbf{v} = (v_1, v_2)^T$, $\mathbf{F} = (f_1, f_2)^T$, and $\mathbf{G}$ is the matrix-integral operator which acts on $\mathbf{v}$ as follows

$$\begin{aligned} \mathbf{G}\mathbf{v} &= \begin{pmatrix} G_{11} & G_{12} \\ G_{21} & G_{22} \end{pmatrix} \begin{pmatrix} v_1 \\ v_2 \end{pmatrix} \\ &= \begin{pmatrix} 0 & \int\limits_{\gamma_2} p(y;x)\ *(y)\, dS_y \\ \int\limits_{\gamma_1} p(x';x)\ *(x')\, dS_{x'} & 0 \end{pmatrix} \begin{pmatrix} v_1 \\ v_2 \end{pmatrix} = \begin{pmatrix} \int\limits_{\gamma_2} p(y;x) v_2(y)\, dS_y \\ \int\limits_{\gamma_1} p(x';x) v_1(x')\, dS_{x'} \end{pmatrix}. \end{aligned} \tag{2.14}$$

The integral equation (2.7) and its equivalent vector counterpart (2.13) with the integral operator $\mathbf{G}$ have nice properties. First of all, the L_1-norm of $\mathbf{G}$ is less than 1, for any configuration of the two overlapping discs, since $\int\limits_{S(x,R)} p(y;x)dS_y = 1$. Hence $(E-\mathbf{G})^{-1}$ exists and is represented as a convergent Neumann series. This also follows from the next assertion which presents a nice property of the Poisson kernel and gives simultaneously an interesting characterization of the Wiener process.

Theorem 2.1. *For any $x \in \gamma_1$ and any $y \in \gamma_2$*

$$\int\limits_{\gamma_2} p(y;x)\,dS_y = \int\limits_{\gamma_1} p(y';y)\,dS_{y'} = 1 - \frac{\theta_1^*}{\pi} - \frac{\theta_2^*}{\pi} = \frac{\theta_{12}^*}{\pi}\,, \tag{2.15}$$

where the angles θ_1^* and θ_2^* are defined as follows (see Figure 2): $2\theta_1^*$ is the angle of view of the arc γ_2 from the centre of the first circle, and $2\theta_2^*$ is the angle of view of the arc γ_1 from the centre of the second circle. The angle $\theta_{12}^* = \pi - \theta_1^* - \theta_2^*$ is the angle of view of the segment (O_1, O_2) from the intersection point P_1 or P_2. This property characterizes the Wiener process as follows. For a Wiener process starting from $x \in \gamma_1$, the probability to reach the arc γ_2 does not depend on the starting point x and is explicitly given by (2.15). Moreover, the same is true for the Wiener process starting from $y \in \gamma_2$: the probability to reach the arc γ_1 is not depending on the starting point y, and is equal to the same constant θ_{12}^*/π given in (2.15).

Proof. Partly, we presented this result in [25]. Here we give a different proof of this elegant result but first let us recall the main idea of the proof in [25]. For any $x \in \gamma_1$ we have obviously:

$$p(y;x) = \frac{\cos(\psi)}{\pi|x-y|} - \frac{1}{2\pi R_1} \tag{2.16}$$

which follows from the relation: $R_1^2 - r_1^2 + |x-y|^2 = 2R_1|x-y|\cos(\psi)$ where ψ is the angle between the vectors $x-y$ and $\mathbf{n}_y$, the inner normal vector at the point y which is collinear to $x_0^{(1)} - y$.

Using the relation (2.16) we can write for any $x \in \gamma_1$:

$$\int\limits_{\gamma_2} p(y;x)\,dS_y = \frac{1}{\pi}\Big\{\int\limits_{\gamma_2} \frac{\cos(\psi)}{|x-y|} dS_y\Big\} - \frac{1}{2\pi R_1}\int\limits_{\gamma_2} dS_y\,.$$

In the right-hand side, the first integral in the braces is the double layer potential integral which is equal (e.g., see [22]) to the angle of view of the arc γ_2 from the point x, i.e., to $(2\pi - 2\theta_2^*)/2$. The second integral is simply θ_1^*/π. This completes the proof, since by symmetry, exactly the same result is obviously obtained for the second disc, when $y \in \gamma_2$.

Let us give another proof of this assertion, based on the series representation of the kernel $p(y;x)$. It is not so elegant as the above proof, but the technique can be used in solving the full eigenvalue problem.

The expansion of the kernel we need is [10]:

$$p(y;x) = \frac{1-\rho^2}{2\pi}\frac{1}{1-2\rho\cos(\theta-\alpha)+\rho^2} = \frac{1}{2\pi} + \frac{1}{\pi}\sum_{k=1}^{\infty}\rho^k\cos[k(\theta-\alpha)]\,. \tag{2.17}$$

Here we use the polar coordinates: the point x is specified by (r,θ), $\rho = r/R$, and the point y - by (R,α).

Let us introduce some notations. The first disc is centered at the origin $O_1 = 0$, and O_2 is the center of the second disc. We denote the point of intersection of the coordinate axes O_1X with the second circle by P_3. Let P_1 and P_2 be the points of intersections of our circles. We introduce the following angles (see

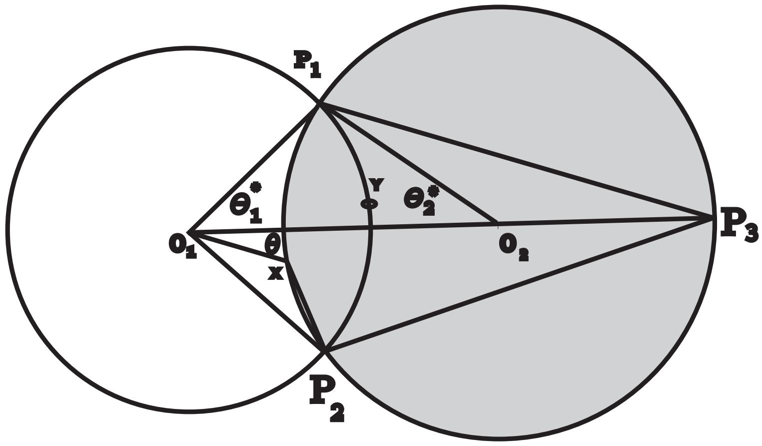

Figure 2: Illustration to the proof of Theorem 2.1.

the picture of Figure 2): ψ_1 is the angle between the vector O_1P_1 and $x-P_1$, and ψ_2 is the angle between the vector O_1P_2 and $x-P_2$. Further, φ_1 is the angle between $x-P_1$ and P_3-P_1; φ_2 is the angle between $x-P_2$ and P_3-P_2.

Routine calculations yield

$$
\begin{aligned}
I &= \int_{-\theta_1^*}^{\theta_1^*} \frac{1-\rho^2}{2\pi}\frac{d\alpha}{1-2\rho\cos(\theta-\alpha)+\rho^2} \\
&= \frac{2\theta_1^*}{2\pi}+\frac{1}{\pi}\sum_{k=1}^{\infty}\rho^k\int_{-\theta_1^*}^{\theta_1^*}\cos[k(\theta-\alpha)]\,d\alpha \\
&= \frac{\theta_1^*}{\pi}+\frac{1}{\pi}\sum_{k=1}^{\infty}\rho^k\left\{\frac{\sin[k(\theta_1^*-\theta)]}{k}+\frac{\sin[k(\theta_1^*+\theta)]}{k}\right\} \\
&= \frac{\theta_1^*}{\pi}+\frac{1}{\pi}\left\{arctg\frac{\rho\sin(\theta_1^*-\theta)}{1-\rho\cos(\theta_1^*-\theta)}+arctg\frac{\rho\sin(\theta_1^*+\theta)}{1-\rho\cos(\theta_1^*+\theta)}\right\}.
\end{aligned}
\tag{2.18}
$$

It is readily seen that

$$
\psi_2 = arctg\frac{\rho\sin(\theta_1^*-\theta)}{1-\rho\cos(\theta_1^*-\theta)}, \quad \psi_1 = arctg\frac{\rho\sin(\theta_1^*+\theta)}{1-\rho\cos(\theta_1^*+\theta)}\,. \tag{2.19}
$$

Simple geometric analysis shows that $\theta_1^*+\theta_2^*/2+\psi_1+\varphi_1=\pi$, $\theta_1^*+\theta_2^*/2+\psi_2+\varphi_2=\pi$, and $\varphi_1+\varphi_2=\pi$. This yields $\psi_1+\psi_2=\pi-2\theta_1^*-\theta_2^*$, which, in view of (2.18), (2.19) completes the proof.

In constructions of iterative numerical procedures, we will need the information about the principal eigenvalue of the integral operator. In the next theorem we find this eigenvalue explicitly. This result was formulated in [25], however the proof there was incomplete. We give here the revised version of the proof.

Theorem 2.2. *The integral operator* $\mathbf{G}$ *is a Fredholm operator with the kernels* $p(y;x)$, $p(x';y)$, *continuous on* $x\in\gamma_1$, $y\in\gamma_2$, *with integrable singularities at the points of intersection of* γ_1 *and* γ_2 *of the type* $p(y;x)\simeq\frac{\sin(\theta_1^*+\theta_2^*)}{\pi|x-y|}$ *as* $x\to y$. *The eigenvalues of* $\mathbf{G}$, λ_i, *are all real, and moreover,* $\lambda_i=\pm\sigma_i\rho(\mathbf{G})$ *where* $\sigma_i\le 1$ *are some positive constants, and* $\rho(\mathbf{G})$ *is the spectral radius of* $\mathbf{G}$ *given explicitly by*

$$
\rho(\mathbf{G}) = 1-\frac{\theta_1^*}{\pi}-\frac{\theta_2^*}{\pi}=\frac{\theta_{12}^*}{\pi}\,.
$$

The integral equation (2.13) has a unique solution which solves the Dirichlet problem (2.1).

Proof. First let us show that the singularities have the form $p(y;x) \simeq \frac{\sin(\theta_1^*+\theta_2^*)}{\pi|x-y|}$ as $x \to y$. Simple geometrical considerations show that $R_1^2 - r^2 = |x-y| \cdot b$, where $b = |x-y^*|$, and y^* is the second point of intersection of the line $x-y$ with the circle $S(x_0, R_1)$. Thus $p(y;x) = \frac{b}{2\pi R_1 |x-y|}$. Now, as $x \in \gamma_1 \to y \in \gamma_2$, we have asymptotically $b \simeq 2R_1 \sin(\theta_1^* + \theta_2^*)$.

Let us now consider the eigenvalue problem. Note that the integral operator $\mathbf{G}$ is not symmetric, but we can symmetrize it if we follow the symmetrization we used above. Indeed, introducing the new functions

$$w_1(x) = v_1(x) \times \sqrt{\frac{R_1}{R_1^2 - |x - x_0^{(1)}|^2}}, \quad w_2(x) = v_2(x) \times \sqrt{\frac{R_2}{R_2^2 - |x - x_0^{(2)}|^2}}$$

we come to the eigenvalue problem for the symmetric integral equation

$$\lambda \mathbf{w} = \bar{\mathbf{G}} \mathbf{w}$$

where the matrix-integral operator $\bar{\mathbf{G}}$ is defined by

$$\bar{\mathbf{G}}\mathbf{w} = \begin{pmatrix} 0 & \int\limits_{\gamma_1} \frac{g_{12}(x,y)}{|x-y|^2} *(y)\, dS_y \\ \int\limits_{\gamma_2} \frac{g_{21}(x,y)}{|y-x|^2} *(x)\, dS_x & 0 \end{pmatrix} \begin{pmatrix} w_1 \\ w_2 \end{pmatrix}.$$

Here

$$g_{12}(x,y) = \frac{1}{2\pi} \sqrt{\frac{R_1^2 - |x - x_0^{(1)}|^2}{R_1}} \sqrt{\frac{R_2^2 - |y - x_0^{(2)}|^2}{R_2}},$$

and

$$g_{21}(x,y) = \frac{1}{2\pi} \sqrt{\frac{R_1^2 - |y - x_0^{(1)}|^2}{R_1}} \sqrt{\frac{R_2^2 - |x - x_0^{(2)}|^2}{R_2}}.$$

So our system of integral equations is symmetric since $g_{12}(x,y) = g_{21}(y,x)$, and hence, the eigenvalues λ are real, moreover, they are concentrated in the interval $(-\rho, \rho)$ symmetrically relative to the origin, where $\rho = \rho(\mathbf{G}) < 1$ is the spectral radius. Indeed, if λ is an eigenvalue with the corresponding eigenfunction (w_1, w_2), then $-\lambda$ is also an eigenvalue with the corresponding eigenfunction $(w_1, -w_2)$.

Let us now evaluate the spectral radius of our system of integral equations. Taking the eigenfunction as a constant $(1,1)^T$, we see that the corresponding eigenvalue is given by

$$\lambda_0 = \int\limits_{\gamma_i} p(y;x)\, dS_y = 1 - \frac{\theta_1^*}{\pi} - \frac{\theta_2^*}{\pi} = \frac{\theta_{12}^*}{\pi} \tag{2.20}$$

which does not obviously depend on x.

It is not difficult to show that $\rho(\mathbf{G}) = \lambda_0$. Indeed, let λ be an arbitrary eigenvalue, and $(w_1, w_2)^T$ - the corresponding eigenfunction. For any $x \in \gamma_1$ we can write $|\lambda||w_i(x)| \le |w_2(y^*)|\lambda_0$, where y^* is a point where $|w_2|$ reaches its maximum. For any $y \in \gamma_2$ we have analogously: $|\lambda||w_2(y)| \le |w_1(x^*)|\lambda_0$, where x^* is the point of maximum of $|w_1|$. From these two inequalities we get the desired result: $|\lambda|^2 \le \lambda_0^2$. Thus $\rho(\mathbf{G}) = \lambda_0$.

Finally, the equivalence of the integral equation and the Dirichlet problem is obvious: the solution of the Dirichlet problem satisfies the integral equation whose solution is unique. This completes the proof.

2.2 Approximating system of linear algebraic equations

Having the integral equation (2.7) or its symmetric version (2.10), we can construct a standard Random Walk based on the Neumann-Ulam scheme, with the phase space $\gamma_1 \cup \gamma_2$. Moreover, we can also construct different iterative methods, e.g., SOR method, directly for these equations. However for more general domains, it is convenient to deal with discrete Random Walks. To this end, we need to approximate the integral equations by the relevant system of linear algebraic equations.

So let us approximate the system of integral equations (2.13) by a system of linear algebraic equations. We choose a set of nodes $x_1,\dots,x_{m_1+1}$ uniformly on the arc γ_1 and $y_1,\dots,y_{m_2+1}$ on γ_2 generating by the uniform polar angles distributions (the end points are included). These meshes subdivide γ_1 and γ_2 in the set of arches $\gamma_1^{(i)}$, $i=1,\dots,m_1$ and $\gamma_2^{(i)}, i=1,\dots,m_2$, respectively. Of course, the nodes can be chosen not uniformly, say, according to some distribution which generates the nodes more densely around the singular points where the arches do intersect.

Since the Poisson kernel $p(y;x)$ has a singularity, it is convenient to take the approximation in the form:

$$\int\limits_{\gamma_1} p(y;y_k)v_2(y)dS_y = \sum_{i=1}^{m_1+1} p_i^{(1)}(x_i,y_k)v_2(x_i), \quad k=2,\dots,m_2,$$

and analogously,

$$\int\limits_{\gamma_2} p(x';x_k)v_1(x')dS_{x'} = \sum_{i=1}^{m_2+1} p_i^{(2)}(y_i,x_k)v_1(y_i), \quad k=2,\dots,m_1,$$

where

$$p_i^{(1)}(x_i,y_k) = \int\limits_{\gamma_1^{(i)}} p(y;y_k)dS_y\,, \quad p_i^{(2)}(y_i,x_k) = \int\limits_{\gamma_2^{(i)}} p(x';x_k)dS_{x'}\,. \tag{2.21}$$

These coefficients can be evaluated explicitly, using the formula (2.5). The same approximation is used to calculate the right hand sides f_1 and f_2 in all grid points. Thus we come to a discrete approximation of (2.13) in the form of the following system of linear algebraic equations

$$w^{(k)} = \sum_{i=2}^{m_1+m_2} a_{ik}\, w^{(k)} + F^{(k)}, \quad k=1,\dots,m_1+m_2\,, \tag{2.22}$$

or in a matrix form $w = Aw + F$.

Here the column-vector $w=(w_1,w_2)^T$ consists of two column-vectors: w_1, whose components approximate the function v_1, and w_2 approximating the function v_2. The same for the vector F.

Note that the matrix A is a square matrix, it has a 2×2-block form, with zero diagonal blocks, and rectangular blocks A_{12} and A_{21} relating the vectors w_1 and w_2.

We use in our calculations also a slightly different approximation, by applying an appropriate interpolation of the integrated functions v and F, and applying a 12-point refinement Gauss approximation formula in the end points of the arc.

2.3 Extension to domains consisting of a set of overlapping discs

Generalization to connected domains consisting of n arbitrarily overlapping discs is not difficult, the main problem is to choose a convenient numeration of the arches inside the discs. Generally this is a tricky problem but not too difficult for computer implementation. We have written a code which automatically generates a numeration, and the relevant matrix A of the generated system of linear equations.

There are domains for which the structure of the matrix kernel of the system of integral equations is very simple and convenient both for theoretical analysis and computer implementation. For example, assume that each disc is overlapping only with two immediate neighbour discs which are non-overlapping - see Figure 3. The relevant system of integral equations is written in a block matrix form, whose general structure is shown below in (2.25) for the case when the domain is a chain of 5 overlapping discs.

This is a particular example belonging to a more general class of domains which we will call DS_2-domains (DS stands for discs, index 2 means the generated matrix is cyclic of index 2).

Definition. *A DS_2-domain is defined as follows: (1) the domain is a connected union of overlapping discs, (2) each disc may overlap with an arbitrary number of discs but each intersection is a result of overlapping of only two discs, (3) any subset of discs which is a closed family of discs (a chain of successively overlapping discs where the first disc overlaps with the last disc, (e.g., see Figure 6) consists of an even number of discs.*

Property A1. *In a DS_2-domain, the numbering of the arches can be chosen so that the generating matrix kernel G of the integral operator* $\mathbf{G}$ *is a cyclic matrix of order 2 and hence it has the following block form*

$$G = \begin{pmatrix} 0 & G_{12} \\ G_{21} & 0 \end{pmatrix} . \tag{2.23}$$

This numbering of arches we call *a consistent numbering*.

Indeed, the consistent numbering is constructed as follows. Let us index the discs successively following say a clockwise direction, as $1, 2, \ldots, n$. We divide all the discs in two different classes of discs: the first class (say, "red" discs) includes the discs with odd indices $1, 3, 5, \ldots$, and the second class includes the discs (say, "black" discs) with even indices. Now, the numbering of arches is as follows: first we number successively along the chosen direction the arches of the discs belonging to the first class, and then turn, in the last disc, to numbering successively the arches of the discs in the second class. For illustration we show in Figures 5 - 7 examples of DS_2-domains, with the red-black indexation: a simple chain of 5 discs in Figure 5, with the matrix A given schematically in Figure 4, left picture; a closed set of 6 discs in Figure 6, and a more complicated set of 17 discs in Figure 7.

By the construction of the indexation it is clear that the matrix G has the desired block structure (2.23) where G_{12} and G_{21} relate the arches of the first and second groups of discs.

By Property A1, and from the block structure (2.23) the following property readily follows.

Property A2. *Let D be an arbitrary DS_2-domain, with a consistent numbering of the arches, and let us take the decomposition* $\mathbf{G} = \mathcal{L} + \mathcal{U}$ *where $\mathcal{L}$ is the left, and $\mathcal{U}$ the right triangular operators whose matrix kernel is given by (2.23). Then the following equalities are true*

$$(E - \omega\mathcal{L})^{-1} = E + \omega\mathcal{L} \quad and \quad \mathcal{L}^2 = \mathcal{U}^2 = 0, \tag{2.24}$$

where ω is an arbitrary parameter.

This property will be used in Section 4 where we construct a SOR method for solving this kind of linear equations.

To illustrate how different can be the generating matrix for different numbering, we consider the domain consisting of $n = 5$ discs presented in Figure 3. First, let us choose the simplest successive numbering of all arches of our phase space, say, from left to right.

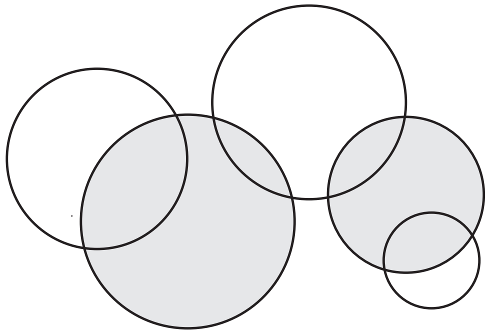

Figure 3: A chain of 5 discs, generating a system of 8 integral equations.

Introducing $k = 2(n-1)$ functions v_i and writing the Poisson formulae in each disc we come to a system of k integral equations $v = \mathbf{G}v + f$ where the kernel of the matrix integral operator $\mathbf{G}$ is a $k \times k$-matrix G which has the following structure: in the first row, only the kernel G_{12} is not zero, the second and the third rows have the following non-zero kernels: G_{21}, G_{24} and G_{31}, G_{34}. The same for the rows 4 and 5: the non-zero entries are G_{43}, G_{46} and G_{53}, G_{56}, etc., so that the j-th' row non-zero entries (j is even) are $G_{j,j-1}$ and $G_{j,j+2}$, while the $j+1$-th' row non-zero entries are $G_{j+1,j-1}$ and $G_{j+1,j+2}$. The last row has only one non-zero entry: $G_{k,k-1}$. So the kernel matrix G has the following structure ($n = 5$ discs, and number of arches $k = 8$):

$$G = \begin{pmatrix} 0 & G_{12} & 0 & 0 & 0 & 0 & 0 & 0 \\ G_{21} & 0 & 0 & G_{24} & 0 & 0 & 0 & 0 \\ G_{31} & 0 & 0 & G_{34} & 0 & 0 & 0 & 0 \\ 0 & 0 & G_{43} & 0 & 0 & G_{46} & 0 & 0 \\ 0 & 0 & G_{53} & 0 & 0 & G_{56} & 0 & 0 \\ 0 & 0 & 0 & 0 & G_{65} & 0 & 0 & G_{68} \\ 0 & 0 & 0 & 0 & G_{75} & 0 & 0 & G_{78} \\ 0 & 0 & 0 & 0 & 0 & 0 & G_{87} & 0 \end{pmatrix}. \tag{2.25}$$

We will show now that to ensure that the system of linear algebraic equations $u = Au + f$ obtained as described above is a good approximation to the exact system of integral equations it is enough to prove that $(E-A)^{-1}$ exists. This in turn is ensured by the fact that our matrices are all substochastic, and their spectral radii are all less than 1.

Let D be a DS_2-domain with the boundary $\Gamma = \partial D$. Let us consider an arbitrary disc of this domain, say, $K(x_k, R_k)$ with $S(x_k, R_k) = \partial K(x_k, R_k)$ which is overlapped with say m_k other discs. Then, $S(x_k, R_k)$ consists of two sets of arches: one set (we denote it by $\tilde{\gamma}_k$) consists of arches lying in the overlappings, and the second one (we denote it by $\tilde{\Gamma}_k$) is a part of the boundary Γ.

Assume that we have fixed some numbering of the arches in our domain D, and the relevant numbering of the functions so that the function $v_j(x)$ is defined on the arc γ_j. This numbering generates a block matrix A whose entries are constructed as follows. Let us fix an arc $\gamma_j \in K(x_k, R_k)$, then the j-th block row consists of m_k non-zero blocks; we denote the integer set of numbering these blocks by J_j, so that $\sum\limits_{l \in J_j}$ means that the sum is taken over all blocks in j-th block row.

Now we estimate the difference between $v_j(x_i)$, the exact solution of the system of integral equations taken on j-th arc at a point $x_i \in \gamma_j$, and the approximation $u_i^{(j)}$ taken as the i-th component of the solution of our linear equation (ith row in the j-th block of the matrix A):

$\varepsilon_i^{(j)} = u_i^{(j)} - v_j(x_i)$. Hence the error vector ε has in j-th block the components $\varepsilon_i^{(j)}$.

Let us also define the error vectors δ and δ^f with entries $\delta_i^{(\tilde{\gamma}_j)}$ and $\delta_i^{(\tilde{\Gamma}_j)}$, the errors of approximation of the Poisson integrals (of the function v and of the boundary function φ, respectively) for j-th arc taken over the set of arches $\tilde{\gamma}_l$ and $\tilde{\Gamma}_l$. Thus we can write for the i-th row in the jth block:

$$\begin{aligned} u_i^{(j)} - v_j(x_i) &= \sum_{l \in J_j} \sum_{k=1}^{n_l} a_{ik}^{(l)} u_k^{(l)} - \sum_{l \in J_j} \int_{\gamma_l} p(y;x_i) v_l(y) dS(y) + \delta_i^{(\tilde{\Gamma}_j)} \\ &= \sum_{l \in J_j} \sum_{k=1}^{n_l} a_{ik}^{(l)} (u_k^{(l)} - v_l(x_k)) + \delta_i^{(\tilde{\gamma}_j)} + \delta_i^{(\tilde{\Gamma}_j)} . \end{aligned}$$

Thus written in the matrix form these relations are

$$\varepsilon = A\varepsilon + \delta + \delta^f . \tag{2.26}$$

Let $\Delta\varphi = \max_i (\varphi_{i+1} - \varphi_i)$ be the maximum difference taken over the all angular meshes. For simplicity we take simple estimations $\|\delta\| < C_1 \Delta\varphi$ and $\|\delta^f\| < C_2 \Delta\varphi$. Therefore, we have

$$\|\varepsilon\| \leq \|(E-A)^{-1}\| \, (C_1 + C_2) \Delta\varphi . \tag{2.27}$$

2.4 Spectral radius estimations

The explicit expression for the spectral radius given in Theorem 2.2 could be obtained only for two overlapped discs. For domains with 3 and more discs, we will get an estimation for the spectral radius of the integral operator of our problem.

Let us first analyze the eigenvalue problem for the system of integral equations (2.13) for a DS_2-domain consisting of three discs, with a consistent numbering of the arches. In this case we have 4 integral equations for the function u_1, u_2, u_3, u_4 defined on the arches $\gamma_1, \gamma_2, \gamma_3$ and γ_4, respectively. Let P be a 4×4 matrix whose non-zero entries are defined by

$$P_{ij} = \int_{\gamma_j} p(y;x) dS_y, \quad x \in \gamma_i, \quad (i,j) = (1,2), (2,1), (2,4), (3,1), (3,4), (4,3).$$

So by definition, P_{ij} is the probability of the transition $x \in \gamma_i \to \gamma_j$, for the pairs of arches $(i,j) = (1,2), (2,1), (2,4), (3,1), (3,4), (4,3)$.

The integrals

$$P_{12} = \int_{\gamma_1} p(y;x) dS_y, \quad P_{43} = \int_{\gamma_3} p(y;x) dS_y,$$

do not depend on the point x, and $P_{12} = P_{21}, P_{34} = P_{43}$, see Theorem 2.1. But P_{24} and P_{31} do depend on the point x. It is not difficult to find a point x^* where P_{24} reaches its maximum $\bar{P}_{24}$; the same for P_{31}.

Indeed, let us denote by x_1 and x_2 the points of intersection of the second and third discs, $S(O_2, R_2)$ and $S(O_3, R_3)$. We construct now a disc $S(O_{23}, R_{23})$ which goes through the points

x_1 and x_2, and touches the first disc at a point $x^* \in \gamma_2$. Then the point x^* is the desired point where P_{24} reaches its maximum $\bar{P}_{24}$. Indeed, of all the points of the arc γ_2, the point x^* is the point with a maximum angle of view of the arc γ_4. As follows from the proof of Theorem 2.1, $\pi P_{24}(x)$ equals the difference between this angle of view and θ^*_{23}, the angle of view of the arc γ_4 from the center O_2. This implies that x^* is indeed the point where $P_{24}(x)$ reaches its maximum. Moreover, by Theorem 2.1, $\bar{P}_{24}$ is equal to $\bar{\theta}_{23}/\pi$ where $\bar{\theta}_{23}$ is the angle of view of the segment (O_2, O_{23}) from the intersection point x_1 or x_2. The same is true for P_{31}: $\bar{P}_{31} = \bar{\theta}_{31}/\pi$.

Let us find the eigenvalues of the matrix $\bar{P}$ which is obtained from P by changing P_{24} and P_{31} with $\bar{P}_{24}$ and $\bar{P}_{31}$, respectively. Simple calculations give

$$\lambda^2_{1,2} = \frac{P^2_{12} + P^2_{34} \pm \sqrt{(P^2_{12} - P^2_{34})^2 + 4P_{12}\bar{P}_{24}P_{43}\bar{P}_{31}}}{2} \,. \tag{2.28}$$

The estimation for any eigenvalue of the eigenvalue problem $\lambda u = \mathbf{G}u$ is now carried out directly, as we have done in the case of two discs: from the first equation we have $|\lambda|\,|u_1(x)| \le P_{12}\,|u_2(y^*)|$ for any x, y^* being the point of maximum of u_2. The value $|u_2(y^*)|$ is estimated from the second equation, etc. Simple calculations yield finally:

$$(\lambda^2 - P^2_{12})(\lambda^2 - P^2_{34}) \le P_{12}\bar{P}_{24}P_{34}\bar{P}_{31}. \tag{2.29}$$

The form of this parabola shows that $\lambda^2_{1,2}$ given by (2.28) are exactly the values where the inequality (2.29) becomes an equality. Thus for any eigenvalue λ we have the estimation: $|\lambda| \le \max_{i=1,2} |\lambda_i|$. This shows that the spectral radius is mainly defined by the value $max\{P_{12}, P_{34}\}$. Indeed, the values $\bar{P}_{24}$ and $\bar{P}_{31}$ are small, compared to P_{12} and P_{34}, as explained above, so we conclude from (2.28) that $\rho(\mathbf{G}) \approx max\{P_{12}, P_{34}\} + \varepsilon$, where ε is a small value.

Analogous estimations can be obtained for the general case of DS_2-domains. For arbitrary connected domains consisting of a finite number of overlapped discs one can use simple estimation

$$\rho(\mathbf{G}) \le \max_{k=1,\dots,n} \sum_{j=1}^{m} P_{kj} \tag{2.30}$$

where n is the total number of rows, and m is the total number of columns in the system of matrix-integral equations; here it is assumed that for all arches which are not the near neighbours, P_{kj} are changed with a majorant of type $\bar{P}_{kj}$.

3. The system of Lamé equations

In this section we will extend the approach presented in Section 2 to a system of elliptic equations (Lamé equation) governing a static 2D elasticity problem. As mentioned in the Introduction, for elliptic systems, probabilistic representations in the form of an expectation over diffusion processes are not known. We mention some efforts to treat this problem. In [17], a direct generalization of the Walk on Spheres process to the Lamé equation was attempted, however the main problem of divergence there was unperceived. In [2], the authors applied the Malliavian calculus to construct an iterative procedure, but it was also unseen that the variance is increasing to infinity with the number of iterations. Note also that a model to treat a crack problem described in [16] appeals to an analogy with the diffusion limited aggregation but without any convergence analysis.

Suppose a homogeneous isotropic elastic body $D \subset \mathbf{R}^n$ with a boundary Γ is given, whose state in the absence of body forces is governed by the classical static elasticity equation, the Lamé equation, see, e.g., [12], [27]:

$$\Delta \mathbf{u}(x) + \alpha \operatorname{grad} \operatorname{div} \mathbf{u}(x) = 0, \quad x \in D, \tag{3.1}$$

where $\mathbf{u}(x) = (u_1(x_1,\dots,x_n),\dots,u_n(x_1,\dots,x_n))$ is a vector of displacements, whose components are real-valued regular functions. The elastic constant α

$$\alpha = \frac{\lambda + \mu}{\mu}$$

is expressed through the Lamé constants of elasticity λ and μ. It can be expressed through the Poisson ratio $\nu = \lambda/2(\lambda+\mu)$ as follows: $\alpha = 1/(1-2\nu)$. The Poisson ratio characterizes the relative amount of the change of the transverse to longitudinal displacements. It is known that due to thermodynamical reasons ν is bounded between $-1 \le \nu < 0.5$. This implies for α: $1/3 \le \alpha < \infty$. So there are materials with negative values of ν (α varies in $1/3 \le \alpha \le 1$), and materials with $\nu \approx 0.5$. The last case is very difficult for computational treating.

The first boundary value problem for the Lamé equation consists in finding a vector function $\mathbf{u} \in C^2(D) \cap C(\bar{D})$ satisfying the boundary condition

$$\mathbf{u}(y) = \mathbf{g}(y), \quad y \in \Gamma\,, \tag{3.2}$$

where $\mathbf{g} \in C(\Gamma)$ is a given vector-function.

In a full analogy with the Laplace equation, we will use the integral formulation of the given boundary value problem which is based on the spherical mean value relation which is a generalized Poisson formula. In what follows we deal with the two-dimensional case.

Let us consider an arbitrary point $x = (x_1,x_2)$ with polar coordinates (r,φ') inside a disk $K(x_0,R)$ centered at $x_0 = (x_{01},x_{02})$. The point $y = (y_1,y_2)$ situated on the circle $S(x_0,R)$ has the coordinates (R,θ), where $\theta = \varphi' + \beta$, and z is defined by $z = y - x$, β is the angle between the vectors x and y; ψ is the angle between x and z. Define also the angle φ by $\varphi = \varphi' + \psi$. The following statement given in [27] is a generalization of the Poisson formula:

Theorem 3.1. *The solution to the equation (3.1) satisfies the following mean value relation, x being an arbitrary point in $K(x_0,R)$:*

$$u_i(x) = \frac{R^2 - |x-x_0|^2}{2\pi R} \sum_{j=1}^{2} \int\limits_{S(x_0,R)} \frac{b_{ij}(x,y)\,u_j(y)}{|x-y|^2}\, dS_y\,, \quad i = 1,2, \tag{3.3}$$

where b_{ij} are functions of x,y, explicitly represented as the entries of the following matrix

$$B = \frac{\alpha}{\alpha+2}\begin{pmatrix} \frac{2}{\alpha} + 2\cos^2\varphi + \frac{|x-y|}{R}\cos(\theta+\varphi) & 2\cos\varphi\sin\varphi + \frac{|x-y|}{R}\sin(\theta+\varphi) \\ 2\cos\varphi\sin\varphi + \frac{|x-y|}{R}\sin(\theta+\varphi) & \frac{2}{\alpha} + 2\sin^2\varphi - \frac{|x-y|}{R}\cos(\theta+\varphi)\,. \end{pmatrix}$$

Since by definition we have

$$\cos\theta = \frac{y_1 - x_{01}}{R}, \quad \sin\theta = \frac{y_2 - x_{02}}{R}, \quad \cos\varphi = \frac{y_1 - x_1}{|x-y|}, \quad \sin\varphi = \frac{y_2 - x_2}{|x-y|},$$

we get

$$b_{11} = 1 + \frac{\alpha}{\alpha+2}\left[\frac{(y_1-x_1)^2 - (y_2-x_2)^2}{|x-y|^2} + \frac{(y_1-x_1)(y_1-x_{01}) - (y_2-x_2)(y_2-x_{02})}{R^2}\right],$$

$$b_{22} = 1 - \frac{\alpha}{\alpha+2}\left[\frac{(y_1-x_1)^2 - (y_2-x_2)^2}{|x-y|^2} - \frac{(y_1-x_1)(y_1-x_{01}) - (y_2-x_2)(y_2-x_{02})}{R^2}\right],$$

$$b_{12} = b_{21} = \frac{\alpha}{\alpha+2}\left[2\frac{(y_1-x_1)(y_2-x_2)}{|x-y|^2} + \frac{(y_2-x_2)(y_1-x_{01}) + (y_1-x_1)(y_2-x_{02})}{R^2}\right].$$

In the notation of $p(y;x)$ introduced in (2.4), the relation (3.3) reads in the matrix form:

$$\mathbf{u}(x) = \int\limits_{S(x_0,R)} p(y;x)\, B\mathbf{u}(y)\, dS(y)\ . \tag{3.4}$$

Taking this representation for two overlapping discs (see Figure 1), we can derive a system of 4 integral equations defined on the arches γ_1 and γ_2. Indeed, let us introduce the notations: $v_1^{(1)}(x) = u_1(x)$ and $v_1^{(2)}(x) = u_2(x)$ for $x \in \gamma_1$, and $v_2^{(1)}(x) = u_1(x)$ and $v_2^{(2)}(x) = u_2(x)$ for $x \in \gamma_2$. Then the analog of the system (2.13) can be written as $\mathbf{v} = \mathbf{G}\mathbf{v} + \mathbf{F}$, or in more details,

$$\begin{pmatrix} v_1^{(1)} \\ v_1^{(2)} \\ v_2^{(1)} \\ v_2^{(2)} \end{pmatrix} = \begin{pmatrix} 0 & 0 & B_{11} & B_{12} \\ 0 & 0 & B_{21} & B_{22} \\ \hat{B}_{11} & \hat{B}_{12} & 0 & 0 \\ \hat{B}_{21} & \hat{B}_{22} & 0 & 0 \end{pmatrix} \begin{pmatrix} v_1^{(1)} \\ v_1^{(2)} \\ v_2^{(1)} \\ v_2^{(2)} \end{pmatrix} + \begin{pmatrix} f_1^{(1)} \\ f_1^{(2)} \\ f_2^{(1)} \\ f_2^{(2)} \end{pmatrix} \tag{3.5}$$

where the integral operators B_{ij}, $i,j = 1,2$ are defined, according to (3.3), for the points of the first disc $x \in K(x_0^{(1)}, R_1)$:

$$B_{ij} v_2^{(j)}(x) = \int\limits_{\gamma_2} p(y;x)\, b_{ij}(x,y)\, v_2^{(j)}(y)\, dS(y), \quad i,j = 1,2\ ,$$

while the integral operators $\hat{B}_{ij}$, $i,j = 1,2$ are defined for the points of the second disc $x \in K(x_0^{(2)}, R_2)$:

$$\hat{B}_{ij} v_1^{(j)}(x) = \int\limits_{\gamma_1} p(y;x)\, b_{ij}(x,y)\, v_1^{(j)}(y)\, dS(y), \quad i,j = 1,2\ .$$

The functions f_i^j are defined analogously:

$$f_i^{(j)}(x) = \sum_{k=1}^{2} \int_{\Gamma_i} p(y;x)\, b_{jk}(x,y)\, g_k(y)\, dS(y), \quad i,j = 1,2 \; .$$

It should be noted that the equivalence of the system (3.5) and the boundary value problem (3.1), (3.2) is not evident, in contrast to the case of the Laplace equation. Indeed, the L_1-norm of the integral operator is generally larger than 1, so we have to use finer properties. Indeed, let us estimate the L_1-norm. Simple evaluations yield:

$$\|\mathbf{G}\|_{L_1} \leq Q_\alpha \left(1 - \frac{\theta_1^*}{\pi} - \frac{\theta_2^*}{\pi}\right) \tag{3.6}$$

where

$$Q_\alpha = \frac{2 + 4\sqrt{2}\alpha}{\alpha + 2} \; . \tag{3.7}$$

In the general case of a DS_2-domain we obtain by (2.30)

$$\|\mathbf{G}\|_{L_1} \leq Q_\alpha \max_{k=1,\ldots,n} \sum_{j=1}^{m} P_{kj} \; . \tag{3.8}$$

This estimation shows that $\|\mathbf{G}\|_{L_1}$ can be made less than 1 for a fixed value of α by a proper choice of $\theta_1^*, \theta_2^*, \ldots, \theta_n^*$ which would imply a restriction of the overlapping configuration. To be free of such a restriction, we turn to the spectral radius estimation.

Theorem 3.2. *The integral operator* $\mathbf{G}$ *of the system (3.5) is a Fredholm operator with kernels continuous on* $x \in \gamma_1$ *and* $y \in \gamma_2$*, with the same type of singularities at the points of intersections of the arches* γ_1 *and* γ_2 *as the singularities in the case of Laplace equation. The spectral radius of* $\mathbf{G}$ *is less than* 1 *for any nonempty overlapping, which ensures the equivalence of the system (3.5) and the boundary value problem (3.1), (3.2).*

Proof. The first part of the statement immediately follows from the fact that the kernel functions of the integral operator $\mathbf{G}$ are represented as products of bounded functions b_{ij} and the function $p(y;x)$. The property $\rho(\mathbf{G}) < 1$ can be derived as a consequence of the result obtained by Sobolev in [30]: the Schwarz alternation procedure for two overlapped domains, for the boundary value problem (3.1), (3.2), constructed by the simple iteration of the Green formula representations for these domains, is convergent. For details of this derivation see [27].

Note that it seems quite plausible that Sobolev's arguments hold true for arbitrary connected domains consisting of a finite number of overlapping discs, see [11].

The discrete approximation of the system of integral equations (3.4) in the form of a linear system of algebraic equations is straightforward: using exactly the same nodes we obtain an analog of (2.22). The error vector will have also the same form (2.26), with the estimation of type (2.27). This follows from the structure of the kernel (3.4) represented as a product of the Laplace kernel $p(y;x)$ and smooth functions $b_{ij}(x,y)$. The difference with the Laplace equation is in the entries: instead of a scalar element a_{ij} we have a 2x2 matrix $\{b_{ij}\}$. So all the stochastic iteration procedures we present in the next sections are equally applicable to systems of linear algebraic equations generated by both the Laplace and Lamé integral kernels.

The principal difference of the Laplace and Lamé integral kernels is that the system of algebraic equations generated by the Lamé integral kernel is not substochastic, in contrast to the case of the Laplace integral kernel.

4. Monte Carlo Iteration methods

In this section we present different Monte Carlo iterative procedures for solving linear systems of equations, generally being integral equations, with specific details for system of linear algebraic equations. First we present a general iterative procedure with random parameters which in the deterministic limit tends to the iterative procedure with Chebyshev parameters. In the next subsection we describe a randomized version of the successive over relaxation (SOR) type method. Both classes of methods will be used then to solve our systems of linear equations.

4.1 A generalized Vorobiev's stochastic iterative procedure with optimal random parameters

Assume we have to solve a linear, generally, integral equation of the second kind:

$$u(x) = \int\limits_X k(x,y)u(y)dy + f(x) \tag{4.1}$$

or in the operator form $u = Ku + f$.

Standard Monte Carlo algorithms (known also as the Neumann-Ulam scheme) for solving this kind of equations usually require that $\rho(|K|) < 1$, where the integral operator $|K|$ is defined by its kernel $|k(x,y)|$, $\rho(|K|)$ is the spectral radius. Sabelfeld (see [21], and [22]) has extended the Neumann-Ulam methods by applying conformal transformation of the spectral parameter. This generates different iteration procedures which are convergent even if $\rho(|K|) \geq 1$. However the main problem - the variance finiteness of the relevant Monte Carlo estimator - was resolved under certain restrictive assumptions. Further developments of this approach can be found in [14].

Here we suggest to use a nonstationary iterative procedure, starting with $u_0 = 0, u_1 = \beta_0 f$:

$$u_{j+1} = \alpha_j u_j + \beta_j (f + Ku_j), \quad j = 1, \ldots, \tag{4.2}$$

where α_j, β_j are some constants which we choose so that $\alpha_j + \beta_j = 1$.

It should be stressed that we will deal here with two stochastic elements in the Monte Carlo evaluation of the iterative procedure (4.2): the first one introduced by Vorobiev [31] suggests to sample the parameters β_j at random, according to a certain optimal probability distribution. The second one is introduced by a Markov chain for a Monte Carlo calculation of the iterations K^j. Of course, these two elements can be used independently. For instance, in [31] the random parameters were used to solve linear algebraic iterations where the matrix iteration A^j were calculated directly. On the other side, in our first algorithms, we have constructed a numerical procedure where in (4.2), the iterations K^j were calculated by a Markov chain simulation, while the parameters were deterministic, satisfying a convergence condition (see below (4.4)).

Simple analysis shows that if we assume that the eigenfunctions ϕ_l (defined through $\phi_k = \lambda_k K \phi_k$) form a complete system in the space $L_2(X)$ of square-integrable functions on a space X, then the following estimation of the error can be made.

Let the initial error be $\varepsilon_0 = \sum_{i=1}^{\infty} c_i \phi_i$, then

$$\varepsilon_n = \sum_{i=1}^{\infty} c_i \left[\prod_{j=1}^{n} (\alpha_j + \beta_j \lambda_i^{-1}) \right] \phi_i = \sum_{i=1}^{\infty} c_i \left[\prod_{j=1}^{n} \left(1 - \beta_j \frac{\lambda_i - 1}{\lambda_i} \right) \right] \phi_i \,. \tag{4.3}$$

Hence if for all λ_i there exists a set of numbers β such that

$$\left| 1 - \beta \frac{\lambda_k - 1}{\lambda_k} \right| = q_k < 1 - \delta, \quad \delta > 0 \tag{4.4}$$

then for all β_j belonging to this set the method converges.

Algorithm NIRP: Nonstationary Iterations with Random Parameters.

It is possible to construct different Monte Carlo estimators following this iterative procedure. We prefer to construct biased estimators: first, we fix n, the number of iterations we will perform, and choose the numbers $\beta_0, \beta_1, \ldots, \beta_{n-1}$ at random. How to make such a choice optimal, we will discuss later.

Then we proceed as follows. We use for convenience the reversed indexation, so let $\beta'_k = \beta_{n-k}$, $k = 1, \ldots, n$. First we choose $p(x,y)$, an arbitrary transition density function for our Markov process such that $p(x,y) \neq 0$ for (x,y) where $k(x,y) \neq 0$. Start our Markov chain from the point where the solution $u(x_0)$ should be found, say, x_0, and take the current state as $X = x_0$. The current value of the iteration index is $j = 1$. Take the initial value of the weight as $Q = 1$. The initial value of the random estimator is $\xi = f(x_0)\,\beta'_1$. Then, make the following steps:

1. Sample uniformly in $(0,1)$ a random number *rand* and check if *rand* $> \beta'_j$. If so, then calculate the random estimator

   $$\xi := \xi + Q f(X)\,\beta'_{j+1} \,,$$

   and go to the next iteration which means that we put $j := j+1$ and go to 1 (provided $j < n$).

2. Otherwise if *rand* $\leq \beta'_j$, we simulate the transition from the current state X to the next state Y according to the transition density $p(x,y)$. Then recalculate the weight $Q := Qk(X,Y)/p(X,Y)$, and the random estimator is scored as $\xi := \xi + Q\beta'_{j+1} f(Y)$. The current state is now renewed as $i = k$, $X = Y$; we turn to the next iteration again by putting $j := j+1$ and go to 1 if $j < n$.

After n steps we finish the evaluation of our random estimator $\xi(x_0)$. It is not difficult to show that the constructed random estimator ξ is unbiased:

$$u_n(x_0) = E\xi \,.$$

Indeed, for $i = 1, 2$ this is obvious since $u_0 = 0$, $u_1 = \beta_0 f$. The next step is also the next step in the Markov chain method since

$$u_{j+2} = (\alpha_{j+1}E + \beta_{j+1}K)(\alpha_j E + \beta_j K)u_j + (\alpha_{j+1}E + \beta_{j+1}K)\beta_j f + \beta_{j+1}f,$$

and so on. After n steps we will have

$$\begin{aligned} u_{j+n} &= \left\{ \prod_{i=1}^{n} (\alpha_{j+n-i}E + \beta_{j+n-i}K) \right\} u_j \\ &+ \sum_{k=1}^{n-1} \left[\left\{ \prod_{i=1}^{n-k} (\alpha_{j+n-i}E + \beta_{j+n-i}K) \right\} \beta_{j+k-1} f \right] + \beta_{j+n-1} f \ . \end{aligned} \tag{4.5}$$

Written in this form, the iteration procedure can be clearly evaluated as described in the above algorithm.

Optimal random parameters β_k.

As mentioned above, the parameters β_i can be chosen deterministically, say, according to the Chebyshev iteration method which is based on polynomials uniformly close to zero, e.g., see [13]. However in our method, it is quite natural to choose these parameters randomly, according to a minimization of the probabilistic error (see [31]). Remarkably, the Chebyshev choice of parameters will follow from this probabilistic approach.

To analyze the error, it is convenient to work with the operator $H = E - K$. We introduce the corresponding polynomial by

$$P_n(t) = \prod_{i=1}^{n} (1 - \beta_i t) \ . \tag{4.6}$$

By the definition of the iterations (4.2), and taking into account that $\alpha_j = 1 - \beta_j$, $Hu = f$, and $\varepsilon_j = u - u_j$, we readily find that

$$\varepsilon_{j+n} = P_n(H)\varepsilon_j \ . \tag{4.7}$$

It is the general idea, in the iterative methods, to make the polynomial $P_n(t)$ as close to zero as possible, and in the deterministic approach the problem was solved by Markov and Chebyshev (e.g., see [13]).

There is another approach suggested in [31] where the parameters β_k are sampled at random, and it is then natural to measure the error in the probabilistic sense.

So let us assume that we have chosen n random numbers $\beta_1, \ldots, \beta_n$ which are equally and independently distributed on some interval. Then the polynomial P_n is a random variable, and we can write:

$$\ln |P_n| = \sum_{k=1}^{n} \ln p_k \tag{4.8}$$

where $p_k = |1 - \beta_k t|$. Note that the random numbers $\ln p_k$ are equally and independently distributed, so we can apply the central limit theorem. This implies that as n increases, the distribution density function of $\ln |P_n|$ tends to a Gaussian distribution density

$$K(x) = \frac{1}{\sqrt{2\pi n D}} \exp\left\{ -\frac{(x - na)^2}{2nD} \right\}$$

where $a = \langle \ln|1-\beta_k t| \rangle$ is the expectation, and D - the variance of $\ln p_k$. Standard considerations yield

$$P\Big(|P_n| > \varepsilon\Big) \approx 1 - \Phi\left(\frac{\ln(\varepsilon) - na}{\sqrt{2nD}}\right)$$

where Φ is the function $\Phi = \frac{2}{\sqrt{\pi}} \int_0^x e^{-t^2}\, dt$. From this follows that to ensure that the probability of deviation of $P_n(t)$ tends to zero we have to require that the expectation a is negative.

Let $\varphi(x)$ be the distribution density of β_k which is defined on the interval $[M^{-1}, m^{-1}]$ where m and M are the lower and upper boundaries of the spectrum of the operator $E - K$. Thus we have

$$a = \int_{1/M}^{1/m} \ln|tx-1|\, \varphi(x)\, dx \quad D = \int_{1/M}^{1/m} (\ln|tx-1| - a)^2\, \varphi(x)\, dx\,. \tag{4.9}$$

In [31] it is suggested that the expectation a should not depend on t, which implies that

$$\frac{da}{dt} = \int_{1/M}^{1/m} \frac{x\varphi(x)}{tx-1}\, dx = 0\,. \tag{4.10}$$

A density function on $[M^{-1}, m^{-1}]$ which solves (4.10) has the form:

$$\varphi(x) = \frac{1}{\pi x \sqrt{(1-mx)(Mx-1)}}\,. \tag{4.11}$$

This gives

$$a = -\ln \frac{\sqrt{M} + \sqrt{m}}{\sqrt{M} - \sqrt{m}}, \tag{4.12}$$

and

$$D < \pi^2 + 8\ln 2 \sqrt{\frac{m}{M}} + O((\frac{m}{M})^{3/2})\,. \tag{4.13}$$

From this, an estimation of the number of iterations n required to reach the error ε can be derived

$$n > \frac{\ln(\varepsilon)}{a}$$

where the expectation a is given by (4.12).

One might argue that Vorobiev's suggestion to choose the density φ under the condition that the expectation a is independent of t looks unjustified. However in his second paper [32] it was shown that in some sense, this choice cannot be improved.

Sampling from the density φ is simple: by the inversion method we find first the simulation formula for the random number β_k^{-1}, which finally yields

$$\beta_k = \frac{2}{(M-m)\, cos(\pi\, rand_k) + M + m} \tag{4.14}$$

where $rand_k$ are random numbers uniformly distributed on $(0,1)$. A variance reduction can be achieved by the following modification: the interval is uniformly divided into n equal subintervals, and then, change in the simulation formula (4.14) $rand_k$ with $(j - rand_j)/n$ where j are integer numbers which cyclically vary with period n as $j = 1, \ldots, n$, and $rand_j$ are random numbers uniformly distributed on $(0,1)$. Remarkably, if $rand_j$ are changed with their expectations 0.5, we come to the method with optimal Chebyshev parameters, see [31].

4.2 SOR method

Let us start with the simple case of two overlapping discs and the governing system of integral equations (2.13). The matrix kernel $\mathbf{G}$ can be represented as $\mathbf{G} = \mathcal{L} + \mathcal{U}$ where $\mathcal{L}$ and $\mathcal{U}$ are the lower and upper - triangular operators, respectively:

$$\mathcal{L}v = \begin{pmatrix} 0 & 0 \\ \int\limits_{\gamma_1} p(x';y)\,*(x')dS_{x'} & 0 \end{pmatrix} \begin{pmatrix} v_1 \\ \\ v_2 \end{pmatrix} = \begin{pmatrix} 0 \\ \\ \int\limits_{\gamma_1} p(x';y)\,v_1(x')dS_{x'} \end{pmatrix}$$

and

$$\mathcal{U}v = \begin{pmatrix} 0 & \int\limits_{\gamma_1} p(y;x)\,*(y)dS_y \\ 0 & 0 \end{pmatrix} \begin{pmatrix} v_1 \\ \\ v_2 \end{pmatrix} = \begin{pmatrix} \int\limits_{\gamma_2} p(x';y)\,v_2(x')dS_{x'} \\ \\ 0 \end{pmatrix} .$$

Introducing a scalar parameter ω we rewrite our equation $\mathbf{v} = \mathbf{G}\mathbf{v} + \mathbf{F}$ in the form:

$$\mathbf{v} = (E - \omega\mathcal{L})^{-1}[(1-\omega)E + \omega\mathcal{U}]\mathbf{v} + \omega(E - \omega\mathcal{L})^{-1}\mathbf{F} . \tag{4.15}$$

This is a general form of transformation which is used to construct SOR method as a simple iteration method for (4.15) (e.g., see [33] and [13]). Note that in the case we consider here, i.e., for DS_2-domains, with a consistent numbering of arches, $(E - \omega\mathcal{L})^{-1} = E + \omega\mathcal{L}$, therefore, our equation has the following simple form

$$\mathbf{v} = \mathbf{T}_\omega \mathbf{v} + \mathbf{d} \tag{4.16}$$

where

$$\mathbf{T}_\omega = (E + \omega\mathcal{L})[(1-\omega)E + \omega\mathcal{U}], \quad \mathbf{d} = \omega(E + \omega\mathcal{L})\mathbf{F} .$$

Now we notice that all this is true for any DS_2-domain, since here we have used only (2.24), the Property A2, which holds for such domains.

Now, if $\rho(|\mathbf{T}_\omega|) < 1$, we can apply the standard Neumann-Ulam scheme. It can be applied directly to the integral form, or to the approximating system of linear algebraic equations. Here it is convenient again to use a Markov chain of length n, to evaluate the n-th approximation.

Note that in the case of matrix operators, there are well known interrelations between the spectra of $\mathbf{G}$ and $\mathbf{T}_\omega$, (e.g., see [33], [18], [8]) which can be used to analyse the convergence and variance of stochastic methods. Here we show an analogous result for integral operators.

Theorem 4.1. *Assume that D is an arbitrary DS_2-domain. The eigenvalues λ_T of the integral operator $\mathbf{T}_\omega$ and the eigenvalues μ of the original integral operator $\mathbf{G} = \mathcal{L} + \mathcal{U}$ are related by*

$$(\lambda_T + \omega - 1)^2 = \lambda_T\,\omega^2\mu^2 . \tag{4.17}$$

Hence, for each i, the two numbers

$$\lambda^{\pm}_{T,i} = \left\{ \frac{\omega\mu_i \pm \sqrt{\omega^2\mu_i^2 - 4(\omega-1)}}{2} \right\}^2 = 1 - \omega + \frac{\mu_i^2\omega^2}{2} \pm \frac{\mu_i\omega}{2}\sqrt{\mu_i^2\omega^2 + 4 - 4\omega} \tag{4.18}$$

are eigenvalues of the operator $\mathbf{T}_\omega$.

Proof. In the transformations below we use the property (2.24) which is true for an arbitrary DS_2-domain. Simple transformation of the eigenvalue problem

$$\mathbf{T}_\omega \mathbf{v} = \lambda_T \mathbf{v}$$

yields:

$$(1-\omega-\lambda_T)E\mathbf{v} + \omega\,\mathcal{U}\mathbf{v} + \lambda_T\,\omega\,\mathcal{L}\mathbf{v} = 0,$$

hence,

$$(\mathcal{U}+\lambda_T\,\mathcal{L})\mathbf{v} = \frac{\lambda_T+\omega-1}{\omega}\mathbf{v}\,. \tag{4.19}$$

Second iteration of (4.19) results in

$$(\mathcal{U}+\lambda_T\,\mathcal{L})^2\mathbf{v} = \lambda_T(\mathcal{U}\mathcal{L}+\mathcal{L}\mathcal{U})\mathbf{v} = \Big(\frac{\lambda_T+\omega-1}{\omega}\Big)^2\mathbf{v}\,. \tag{4.20}$$

Note that the second iteration of the original eigenvalue problem $(\mathcal{L}+\mathcal{U})\,\mathbf{w} = \mu\,\mathbf{w}$ reads:

$$(\mathcal{U}+\mathcal{L})^2\mathbf{w} = (\mathcal{L}\mathcal{U}+\mathcal{U}\mathcal{L})\,\mathbf{w} = \mu^2\,\mathbf{w}. \tag{4.21}$$

Comparison of (4.20) and (4.21) yields

$$\frac{1}{\lambda_T}\Big(\frac{\lambda_T+\omega-1}{\omega}\Big)^2 = \mu^2 \tag{4.22}$$

which proves (4.17). The relation (4.18) follows immediately from (4.17).

It is well known (e.g., see [33]) that the necessary condition for the convergence of the SOR method is $|\omega-1|<1$, and the minimum of λ_T is attained at

$$\omega_{opt} = \frac{2}{1+\sqrt{1-\rho^2(\mathbf{G})}}\,. \tag{4.23}$$

Moreover, for any ω in the range $0<\omega<2$,

$$\rho(\mathbf{T}_\omega) = \begin{cases} \Big[\omega\rho(\mathbf{G}) + \sqrt{\omega^2\rho^2(\mathbf{G}) - 4(\omega-1)}\Big]^2/4 & if\ \ 0<\omega\le\omega_{opt}, \\ \omega-1 & if\ \ \omega_{opt}\le\omega<2\,. \end{cases} \tag{4.24}$$

We will use the relation (4.18) to estimate the variance of our stochastic algorithm for solving the Lamé equation in Section 5.2.

Remark 4.1. *The estimation (5.6) obtained in the next section and calculations of Section 6 will show that the best results are obtained with a Random Walk method based on the Gauss-Seidel method, i.e., SOR method with* $\omega = 1$, *when* $\rho(\mathbf{T}_\omega) = \rho^2(\mathbf{G})$. *For illustration, we show in Tables 1 and 2 the general structure of the relevant kernel matrices* T_ω *for the case of a* DS_2*-domain consisting of 5 discs (see Figure 5) where* A_{ij} *stand for the relevant kernels of the original system of integral equations.*

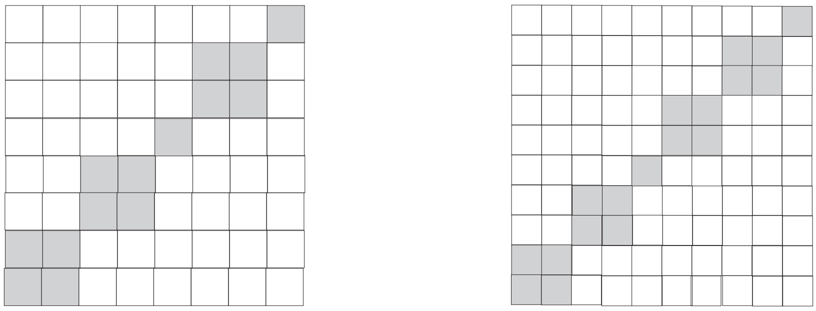

Figure 4: General structure of block matrices for the consistent numbering through “Red-Black” indexation. Left picture: 5 discs shown in Figure 3. Right picture: The same geometry, but for 6 discs.

$$
R_\omega = \left|\begin{array}{cccc||cccc}
0 & 0 & 0 & 0 & 0 & 0 & 0 & \omega A_{18} \\
0 & 0 & 0 & 0 & 0 & \omega A_{26} & \omega A_{27} & 0 \\
0 & 0 & 0 & 0 & 0 & \omega A_{26} & \omega A_{27} & 0 \\
0 & 0 & 0 & 0 & \omega A_{45} & 0 & 0 & 0 \\
\hline
0 & 0 & \omega_2 A_{53} & \omega_2 A_{54} & \omega^2 A_{54} A_{45} & \omega^2 A_{53} A_{36} & \omega^2 A_{53} A_{37} & 0 \\
0 & 0 & \omega_2 A_{63} & \omega_2 A_{64} & \omega^2 A_{64} A_{45} & \omega^2 A_{63} A_{36} & \omega^2 A_{63} A_{37} & 0 \\
\omega_2 A_{71} & \omega_2 A_{72} & 0 & 0 & 0 & \omega^2 A_{72} A_{26} & \omega^2 A_{72} A_{27} & \omega^2 A_{71} A_{18} \\
\omega_2 A_{81} & \omega_2 A_{82} & 0 & 0 & 0 & \omega^2 A_{82} A_{26} & \omega^2 A_{82} A_{27} & \omega^2 A_{81} A_{18}
\end{array}\right|
$$

Table 1: Matrix R_ω in the kernel matrix of SOR: $T_\omega = (1-\omega)E + R_\omega$, for 5 discs shown in Figure 5. Here $\omega_2 = \omega(1-\omega)$.

$$
T_\omega = \left|\begin{array}{cccc||cccc}
0 & 0 & 0 & 0 & 0 & 0 & 0 & A_{18} \\
0 & 0 & 0 & 0 & 0 & A_{26} & A_{27} & 0 \\
0 & 0 & 0 & 0 & 0 & A_{26} & A_{27} & 0 \\
0 & 0 & 0 & 0 & A_{45} & 0 & 0 & 0 \\
\hline
0 & 0 & 0 & 0 & A_{54} A_{45} & A_{53} A_{36} & A_{53} A_{37} & 0 \\
0 & 0 & 0 & 0 & A_{64} A_{45} & A_{63} A_{36} & A_{63} A_{37} & 0 \\
0 & 0 & 0 & 0 & 0 & A_{72} A_{26} & A_{72} A_{27} & A_{71} A_{18} \\
0 & 0 & 0 & 0 & 0 & A_{82} A_{26} & A_{82} A_{27} & A_{81} A_{18}
\end{array}\right|
$$

Table 2: The kernel matrix of the Gauss-Seidel method ($\omega = 1$), for 5 discs shown in Figure 5.

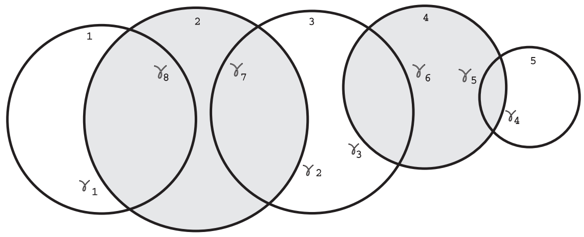

Figure 5: “Red-Black” indexation. A DS_2-domain with 5 discs.

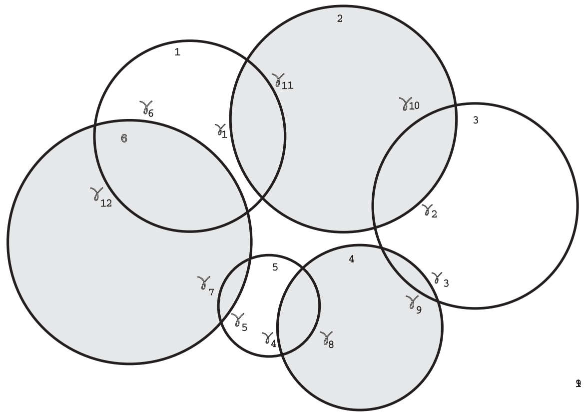

Figure 6: “Red-Black” indexation. A DS_2-domain as a closed chain of 6 discs.

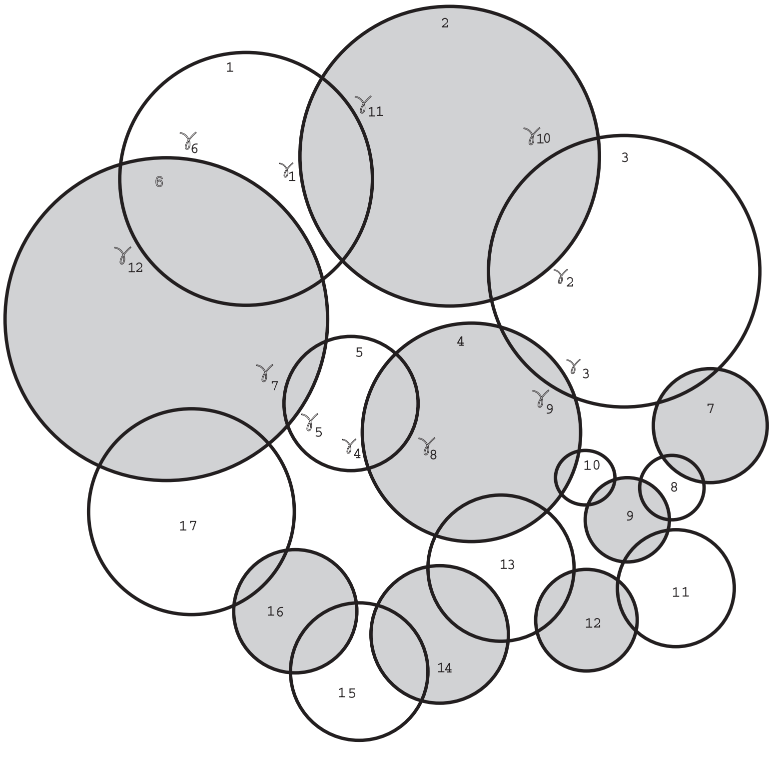

Figure 7: “Red-Black” indexation. A DS_2-domain with 17 discs, which includes 4 closed subsets of even number of discs.

5. Discrete Random Walk algorithms

In this section we present stochastic algorithms for solving systems of linear algebraic equations constructed as discrete approximations to the relevant integral equations, as described in Sections 2 and 3. The stochastic algorithms are based on discrete versions of the iteration methods described in Section 4.1 (iteration method (4.2) with its stochastic implementation in *Algorithm NIRP*, and in Section 4.2 (SOR, based on the transformation (4.16)).

These algorithms can be considered as a Random Walk approach for solving the relevant system of linear algebraic equations on the basis of relevant iteration method which is different from the conventional Monte Carlo method based on the convergent Neumann series.

5.1 Discrete Random Walk based on the iteration method (4.2)

Let us consider a system of linear algebraic equations (LAE) which approximates the relevant system of integral equations for our domain: this can be, e.g., the system of type (2.7) in the case of Laplace equation, or (3.5) - for the Lamé equation. The LAE can be written in its direct form, or in the form related to the appropriate indexation generated by the consistent numbering for the DS_2-domains. We stress that the form of LAE is not important for the stochastic methods we suggest below.

So assume that we have to construct a Monte Carlo algorithm for a system of m linear algebraic equations

$$x_i = \sum_{j=1}^{m} a_{ij} x_j + b_i, \quad i = 1, \dots, m$$

or in the matrix form,

$$x = Ax + b\ . \tag{5.1}$$

We assume that Max, min, the maximal and minimal eigenvalues of the matrix A are known or at least estimated.

Here we adopt the algorithm described in Section 4 for integral equations, to LAE (5.1). We will construct unbiased random estimators ξ_n for u_n, the n-th iteration of the process (4.2) to the solution x, and more precisely, to its l-th component x_l.

First of all, we have to choose a nonnegative transition density matrix $p(i \to j)$; $i, j = 1, \dots, m$, $\sum_{j=1}^{m} p(i \to j) = 1$ for all i, which is consistent with the matrix A, i.e., $p(i \to j) \neq 0$ if $a_{ij} \neq 0$. It is convenient to take

$$p(i \to j) = p_{ij} = \frac{|a_{ij}|}{\sum_{j=1}^{m} |a_{ij}|}\ .$$

This ensures that the random walk will be concentrated only on non-zero elements which is important since we deal with sparse block matrices. We will not have absorptions in our random walk. The Random Walk algorithm can be presented as follows:

0. The initial score is set to zero: $S = 0$.

1. Choose n random parameters according to the formula:

$$\beta(i) = \frac{2}{Max + min + (Max - min)\cos(\pi\, rand(i))}, \quad i = 1, \ldots, n$$

where $rand(i)$, $i = 1, \ldots, n$ are independent samples generated by a rand-generator. Calculate the initial value of the estimator as $\xi_n = b_l \beta(1)$.

2. Set the initial weight $Q = 1$, and the initial number of iteration $j = 1$; fix the initial state as $i = l$.

3. Take a sample $\alpha_j = rand(j)$; if $\alpha_j > \beta(j)$, then calculate $\xi_n := \xi_n + Q b_i \beta(j+1)$, and make the next iteration, i.e., $j := j+1$ and go to p.3 if j, the number of iterations is less than n; otherwise, if $j = n$, make a score $S := S + \xi_n$, and start the new statistics from p.1.

4. Otherwise, if $\alpha_j \leq \beta(j)$, we simulate the transition from the old state i to the new state k according to the density $p(i \to k)$. If the dimension of the problem is very large, we can use the economic algorithm described below in Section 5.2. Recalculate the weight and the random estimator:

$$Q := Q a_{ik}/p_{ik}\ , \quad \xi_n := \xi_n + Q\beta(j+1)\, b_k\ ,$$

then, renew the state as $i = k$, and go to the next iteration, i.e., $j := j+1$, and go to p.3, if j, the number of iterations is less than n; otherwise make a score $S := S + \xi_n$, and start the new statistics from p.1.

Averaging the estimator over statistics of size N gives the result: $x_l \approx S/N$.

5.2 Discrete Random Walk method based on SOR

Here we present two variants of the Random Walk algorithm. Let D be a DS_2-domain, so that $(E - \omega L)^{-1} = E + \omega L$, and hence our system (5.1) can be rewritten in the form

$$x = Tx + f\ , \tag{5.2}$$

where $T = (E + \omega L)((1-\omega)E + \omega U)$, and $f = (E + \omega L)b$.

The first algorithm for calculation of n-th approximation is based on a direct randomized calculation of the finite number of iterations of the operator T, i.e., by evaluation of the Neumann series $f + Tf + T^2 f + \ldots + T^n f + \ldots$. As in the previous section, we do not introduce absorption in our Markov chain. So to calculate the component x_l of the solution to (5.2), we suggest the following algorithm.

0. The initial score is set to zero: $S = 0$.

1. Fix n, the number of iterations to be made, and choose the parameter ω, say, equal to ω_{opt} given by (4.23), or to 1, as in the Gauss-Seidel method. Calculate the matrix T, and the vector f.

2. Set the initial weight $Q = 1$, the number of iteration $j = 1$, and the current state of the Markov chain $i = l$. The initial value of the estimator is set as $\xi_n = f_l$.

3. Simulate the transition from the state i to the new state k according to the density $p(i \to k)$ which is chosen, e.g., as in the method of the previous section:

$$p(i \to k) = p_{ik} = \frac{|t_{ik}|}{\sum_{j=1}^{m} |t_{ij}|} .$$

Racalculate the weight and the random estimator:

$$Q := Q t_{ik}/p_{ik} \ , \quad \xi_n := \xi_n + Q f_k \ ,$$

then, renew the state as $i = k$, and go to the next iteration, i.e., $j := j + 1$, and go to p.3, if j, the number of iterations is less than n; otherwise make a score: $S := S + \xi_n$, and start the new statistics from p.1.

Averaging the estimator over statistics of size N gives the result $x_l \approx S/N$.

Another version of this is algorithm follows from the factorization of the SOR operator. Let $l(i, j)$ and $u(i, j)$ be the entries of the triangular matrices L and U, respectively, and let $al(i, j) = \delta_{ij} + \omega l(i, j)$, $au(i, j) = (1 - \omega)\delta_{ij} + \omega u(i, j)$ where δ_{ij} is the Kronecker symbol. According to the representation $T = (E + \omega L)[(1 - \omega)E + \omega U]$, we make the transition from the state i to state k in two steps: first, sample the transition from i to a state i' according to the matrix $E + \omega L$ (i.e., the transition $i \to i'$ is sampled from the pdf $pl(i, i')$ defined below in (5.3)), and then make the transition $i' \to k$ according to the matrix $((1 - \omega)E + \omega U)$ (i.e., the transition $i' \to k$ is sampled from the pdf $pu(i', k)$ also defined in (5.3)). In each step the weight is recalculated, so that in the first step $Q := Q al(i, i')/pl(i, i')$ and then, $Q := Q au(i', k)/pu(i', k)$, with the final random estimator $\xi_n := \xi_n + Q f(k)$.

The transition densities are defined by

$$pl(i, i') = \frac{|al(i, i')|}{\sum_{j=1}^{m} |al(i, j)|}, \quad pu(i', k) = \frac{|au(i', k)|}{\sum_{j=1}^{m} |au(i', j)|} . \tag{5.3}$$

5.3 Sampling from discrete distribution

In the discrete random walks we use, the discrete distributions p_{ij} are fixed, and therefore, to sample from the discrete distributions, it is very convenient to use the algorithm suggested by Walker (see [19]). We suggest below one of the possible implementations of this method.

So let $p_1, \dots, p_n$ be a discrete distribution.

First, we arrange two arrows: a real array $q_1, \dots, q_n$, and an integer array $a_1, \dots, a_n$. This is done in the following procedure:

1. Let $q_i = p_i n, \quad i = 1,\dots,n$.
2. Construct two initial sets of the set of indices $1,\dots,n$ by $Q = \{i : q_i < 1\}$, $\bar{Q} = \{1,\dots,n\} \setminus Q$.
3. For each element i of Q, do the following: take $j \in \bar{Q}$ and recalculate $q_j := q_j - (1 - q_i)$; put $a_i = j$; if $q_j < 1$ then the set Q is extended by $Q = Q \cup \{j\}$, while $\bar{Q} = \bar{Q} \setminus \{j\}$.
Note that here under "For each element i of Q" we understand that we have to go through all the elements of the continuously renewed set of indices Q.
4. Recalculate $q_i := q_i + i - 1$, $i = 2,\dots,n$.

Having constructed these two arrays, $q_1,\dots,q_n$ and $a_1,\dots,a_n$, the procedure of modelling the required random integer number l from the distribution $p_1,\dots,p_n$ looks simple and uses only one sample of the random generator *rand*, namely:
5. Put $v = n \cdot rand, \quad nn = Int\{v\} + 1$
if $v < q_{nn}$, then $l = nn$, else $l = a_{nn}$.

Note that we arrange the arrays “out of the loop”. This makes the algorithm extremely efficient because the time to sample one transition $i \to k$ does not depend on the dimension of the distribution $p_1,\dots,p_n$. In other words, the computer time is essentially not depending on the number of nodes on the arches we use to approximate the integral equations by a system of linear algebraic equations.

5.4 The variance of stochastic methods

The described algorithms are based on the convergent iteration processes (the nonstationary process (4.2), and the stationary process SOR (4.16)), and on unbiased random estimators of the iterations. However all this does not guarantee that the stochastic method is numerically stable since the variance can be increasing with the number of iterations.

In the nonstationary process, the variance has an estimation (4.13), provided we can control the variance coming from the randomized estimation of each iteration.

Let us consider the variance of the SOR method described in Section 5.2. It is well known (e.g., see [14]) that the Neumann-Ulam scheme for a linear equation $x = Tx + f$ has a finite variance if $\rho(T^2/p) < 1$ where under T^2/p we understand here a matrix whose entries are defined through the entries of the matrix T and the transition probabilities p_{ik} by t_{ik}^2/p_{ik}.

We can derive an estiamtion of the spectral radius $\rho(T^2/p)$ using the form of the transition probabilities we have chosen in our scheme: $p_{ik} = |t_{ik}| / \sum_{j=1}^{m} |t_{ij}|$. Indeed, for such a choice, we have obviously

$$\rho(T^2/p) \leq \|T\|_1 \, \rho(|T|) \tag{5.4}$$

where $\|T\|_1 = \max\limits_{i=1,\dots,m} \sum\limits_{j=1}^{m} |t_{ij}|$, and $|T|$ is a matrix with the entries $|t_{ij}|$.

For the norm $\|T\|_1$, we obtain the estimation

$$\|T\|_1 \leq |1-\omega| + \omega C_1 + \omega|1-\omega| C_2 + \omega^2 C_3 \tag{5.5}$$

where C_1, C_2 and C_3 are some constants expressed through the probabilities P_{ij} and $P_{ik}P_{kj}$. These constants can be expressed through $\|L\|_1$ and $\|U\|_1$. Indeed, from the definition of the matrix T we conclude that $C_2 = \|L\|_1$, $C_1 = \|U\|_1$, and $C_3 = \|L\|_1\|U\|_1$.

For the spectral radius $\rho(|T|)$ we use the expression given by (4.18). Putting these estimations in (5.4) we obtain the desired estimation

$$\rho(T^2/p) \leq \left\{|1-\omega| + \omega C_1 + \omega|1-\omega| C_2 + \omega^2 C_3\right\}\left\{1-\omega+\frac{\mu^2\omega^2}{2} + \frac{\mu\omega}{2}\sqrt{\mu^2\omega^2+4-4\omega}\right\} \tag{5.6}$$

where $\mu = \rho(A)$, A being the original matrix of our linear system.

Note that for two discs, in the case of the Laplace equation, an explicit expression can be obtained: since $\rho(\mathbf{G}) = \lambda_0$, we get for the Gauss-Seidel scheme ($\omega = 1$) $\rho(T^2/p) = \lambda_0^4$.

The behaviour of $\rho(T^2/p)$ on the parameter ω in the general case of an arbitrary DS_2-domain is well described by the estimation (5.6) both for the Laplace and Lamé equations. In the interval $0 < \omega < 1$ it decreases polynomially, with the principal linear term, and for $\omega > 1$ it increases polynomially as well, with the principal term $C_3\rho(\mathbf{G})\,\omega^4$. This is confirmed in our calculations, see Figure 9 (Laplace equation, 5 discs - left panel, and Lamé equation with $\alpha = 5$, for 5 discs - right panel).

6. Numerical simulations

We present first the results of numerical experiments for the Laplace equation which illustrate the convergence acceleration when using the SOR-based RWFS in comparison to the conventional Random Walk on Spheres (RWS) method. Note that under RWS we understand here a discrete random walk on the fixed discs, constructed according to the Neumann-Ulam scheme. The main calculation results however concern the Lamé equation: here we give a detailed numerical analysis of the new methods suggested. In particular, we analyze the behaviour of the spectral radii of the SOR-based integral operators, in particular, how they depend on the parameters ω and α, the rate of overlapping, and the number of discs. For both Laplace and Lamé equations we analyze the error of the method as a function of the number of iterations.

6.1 Laplace equation

The domain consists of four discs of radii 1, all equally pairwise overlapped with $\theta^* = \theta_1^* + \theta_2^* = 0.5$. The Laplace equation is solved by the standard random walk on spheres method (RWS),

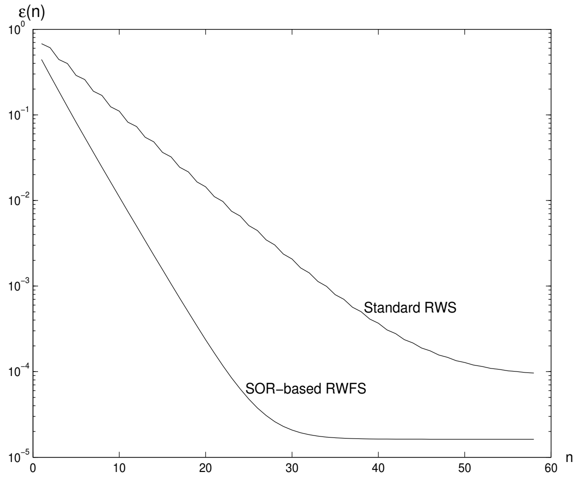

Figure 8: The relative error $\varepsilon(n)$ as a function of n, the number of iterations, for the standard Random Walk on Spheres method (RWS) - upper curve, and for the SOR-based RWFS. Geometry: 4 equal discs of radii 1, all equally pairwise overlapped with $\theta_1^* + \theta_2^* = 0.5$. Laplace equation.

and by the SOR-based RWFS. In Figure 8 we show the relative error ε as a function of the number of iterations. It is clearly seen that the SOR-based RWFS method reaches its steady-state error ε_0 more than 2 times faster than that of standard RWS. In addition, the steady state error ε_0 of the SOR-based RWFS is considerably smaller than that of the standard RWS.

6.2 Lamé equation

The following model boundary value problem is solved:

$$\Delta \mathbf{u}(x) + \alpha \,\mathrm{grad}\,\mathrm{div}\,\mathbf{u}(x) = 0, \quad x \in D, \tag{6.1}$$

with the Dirichlet boundary conditions $\mathbf{u}(y) = \mathbf{g}(y)$, for $y \in \partial D$, the domain D consists of 5 overlapping discs shown in Figure 5. We have chosen the case with the exact solution $u_i(x_1, x_2) = 1 + \frac{1}{2}\frac{\alpha}{1+\alpha}x_i^2 - x_1x_2 + x_j$, $i = 1, 2$, with $j \neq i$.

First we study how the rate of convergence of the SOR-based RWFS depends on the parameter ω. In Figure 9 we show the spectral radii of the following operators: A - the original (untransformed) matrix which generates the standard RWS, with the relevant operator A^2/p, - a matrix with the entries $\{a_{ij}^2/p_{ij}\}$, where p_{ij} is the relevant transition probability. Analogously is defined the matrix T^2/p where T is the matrix of the SOR method. For comparison, in Figure 9 we show the results both for the Laplace (left panel) and Lamé (right panel) equations.

As seen from the results of Figure 9, right panel, the standard RWS diverges in the case of Lamé equation, because $\rho(A^2/p) \approx 1.11$. For the SOR-based RWFS, the spectral radius $\rho(T)$ monotonically decreases with ω, however $\rho(T^2/p)$ reaches its minimum $\rho(T^2/p) \approx 0.6$ at $\omega = 1$. Thus the SOR method with $\omega = 1$, i.e., the Gauss-Seidel method, is optimal here. The

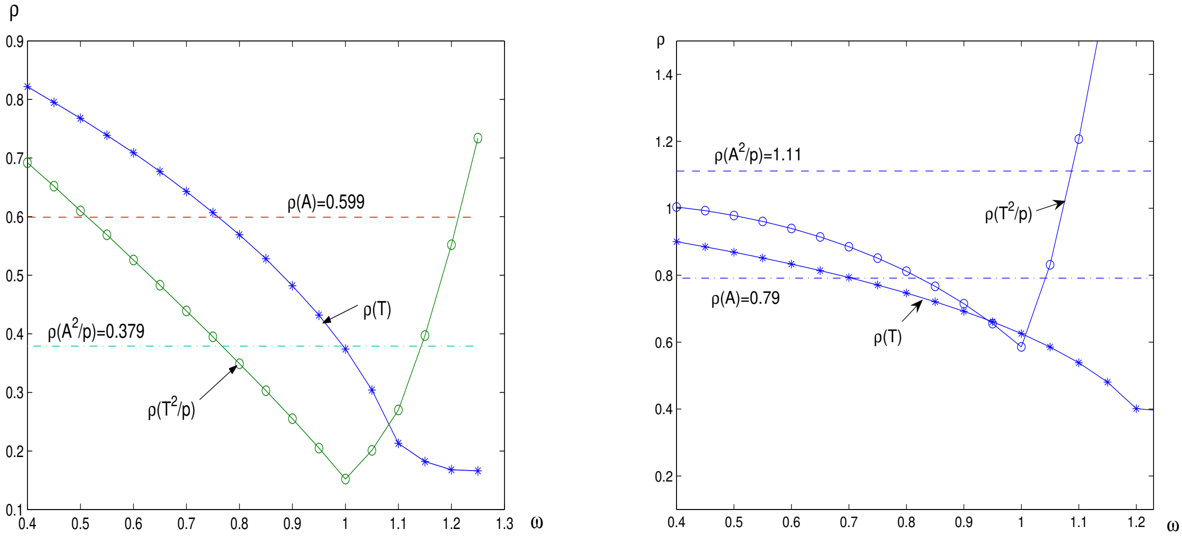

Figure 9: The dependence of the spectral radii $\rho(T)$ and $\rho(T^2/p)$ on the parameter ω. Geometry: 5 discs shown in Fig.5. Left panel: Laplace equation, right panel: Lamé equation, $\alpha = 5$. For comparison, the spectral radii $\rho(A)$ and $\rho(A^2/p)$ are shown where A is the matrix of the untransformed system.

almost linear decrease in the interval $0 \le \omega \le 1$, and the polynomial increase with the principal term of order $C\omega^4$ for $\omega > 1$ are theoretically explained at the end of Section 5.4.

The Gauss-Seidel method has shown the best results in all the calculations, in particular, let us discuss the results presented in Figure 10. Here we show the relative error as a function of the number of iterations. Two cases are considered, left panel: the domain consists of 5 discs shown in Figure 3, and the right panel: 6 discs shown in Figure 6. The Lamé equation was solved by the RWS and SOR-based RWFS methods. It is seen that for both $\alpha = 3.5$ and $\alpha = 6$, the SOR-based RWFS converges, and reaches its steady state error in about 20 iterations. The standard RWS shows a divergence for $\alpha = 6$, while for $\alpha = 3.5$, it shows a kind of stable results, but the error is considerably larger. In Figure 11 it is shown how the spectral radii do depend on the amount of overlapping. Here we have solved the Lamé equation with $\alpha = 2.5$, for two discs of unit radii, and denote $\theta^* = \theta_1^* + \theta_2^*$. It is clearly seen that $\rho(T^2/p) < 1$ for any overlapping while $\rho(A^2/p) < 1$ only if $\theta^* > 1.1$.

A detailed information about the spectral radii is presented in Table 3: here α varies from $1/32$ to 15, the number of overlapping discs is 2, 5, and 10. It is seen that the spectral radii very slowly depend on the number of discs. The dependence on α is more pronounced. It is interesting to note that the standard RWS method diverges after α reaches the value of about 2, while the SOR-based RWFS starts to diverge only after α approaches to 10.

Of course, a question arises if the method can be improved, to guarantee the convergence for larger values of α. For example, it would be quite suggestive to apply the symmetrized version of the SOR method [33] because Q_α in (3.6) varies between 1 and $4\sqrt{2}$, as α increases.

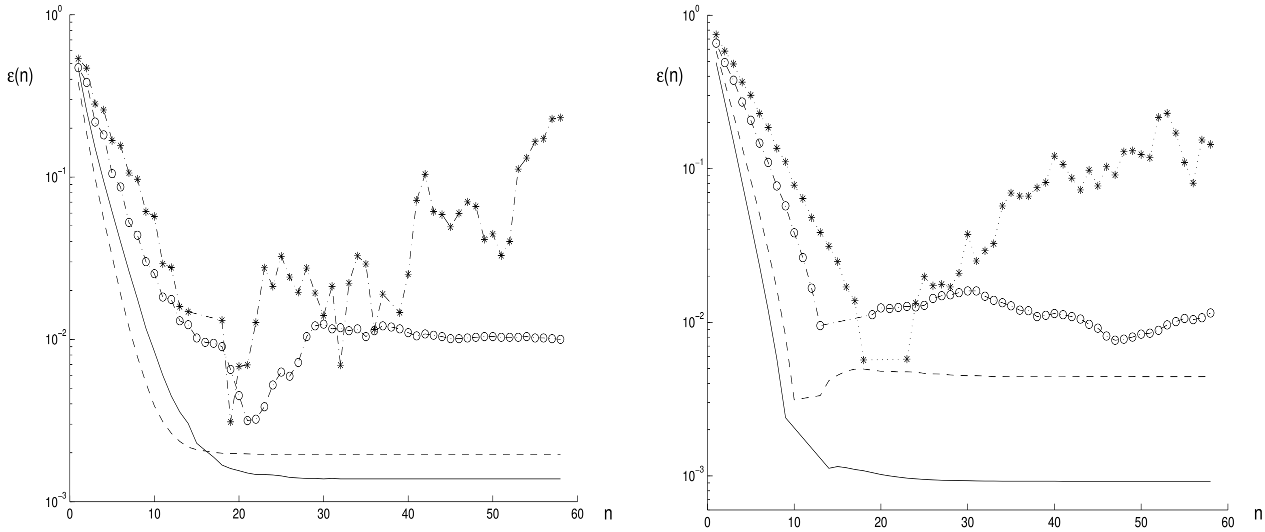

Figure 10: The relative error, as a function of n, the number of iterations. Left panel: the Lamé equation, for 5 discs presented in Fig.3; solid line: SOR, for $\alpha = 3.5$; here the spectral radii are: $\rho(T) = 0.575$, and $\rho(T^2/p) = 0.503$. Dashed line: SOR, for $\alpha = 6$; the spectral radii are: $\rho(T) = 0.65$, and $\rho(T^2/p) = 0.68$. Circles: RWS, for $\alpha = 3.5$; the spectral radii are: $\rho(A) = 0.76$, and $\rho(A^2/p) = 0.99$. Stars: RWS, for $\alpha = 6$; the spectral radii are: $\rho(A) = 0.81$, and $\rho(A^2/p) = 1.17$. Right panel: the same as in left panel, but for 6 discs presented in Fig.4. The spectral radii are: solid line, $\rho(T) = 0.72$, and $\rho(T^2/p) = 0.64$; dashed line, $\rho(T) = 0.79$, and $\rho(T^2/p) = 0.80$; circles: $\rho(A) = 0.85$, and $\rho(A^2/p) = 1.04$; stars: $\rho(A) = 0.89$, and $\rho(A^2/p) = 1.2$.

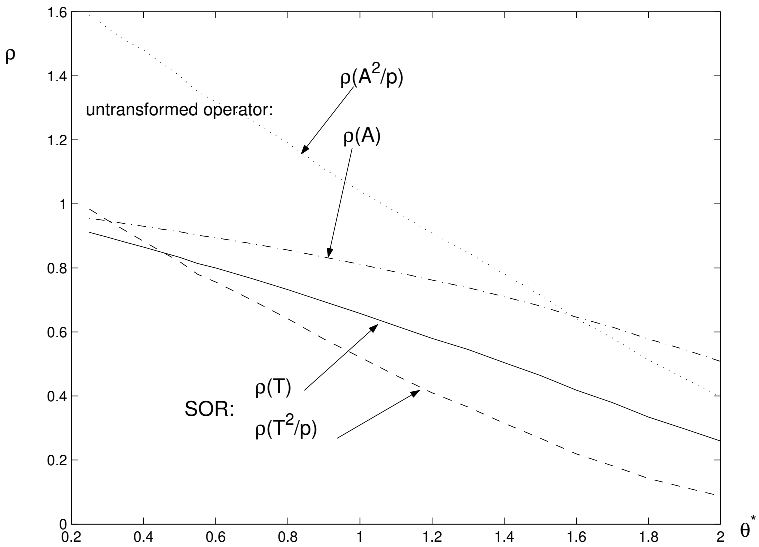

Figure 11: The spectral radii of the SOR operator T, and T^2/p, and for the simple iteration operator A and A^2/p, as functions of θ^*, for two overlapping discs of unit radii. The Lamé equation with $\alpha = 2.5$.

α	N_{discs}	$\rho(T)$	$\rho(T^2/p)$	$\rho(A)$	$\rho(A^2/p)$
$\frac{1}{32}$	2	0.547	0.322	0.740	0.718
	5	0.549	0.333	0.741	0.731
	10	0.536	0.319	0.732	0.713
1.	2	0.569	0.355	0.755	0.783
	5	0.576	0.375	0.759	0.801
	10	0.565	0.361	0.751	0.782
2.5	2	0.662	0.527	0.813	1.06
	5	0.689	0.586	0.830	1.10
	10	0.683	0.574	0.826	1.08
5.	2	0.737	0.705	0.858	1.28
	5	0.781	0.805	0.884	1.34
	10	0.779	0.797	0.883	1.32
9.	2	0.791	0.863	0.889	1.43
	5	0.847	0.997	0.920	1.51
	10	0.853	1.00	0.924	1.51
10.	2	0.799	0.890	0.894	1.46
	5	0.854	1.02	0.924	1.54
	10	0.859	1.02	0.927	1.51
15.	2	0.826	0.983	0.909	1.54
	5	0.890	1.14	0.944	1.62
	10	0.898	1.15	0.947	1.63

Table 3: The spectral radii of the simple iteration operators A and A^2/p, and the SOR operators T, and T^2/p, for different values of the elasticity parameter α, for DS_2-domains consisting of 2, 5 and 10 discs. It is seen that the standard RWS diverges already for $\alpha = 2.5$ even for two discs. The SOR-based RWFS converges in this case for all $\alpha \leq 15$, and for 10 discs, for $\alpha < 9$.

7. Conclusion and discussion

Random Walk on Fixed Spheres method (RWFS) is developed for Laplace and systems of Lamé equations. The method is especially efficient for 2D domains represented as a family of overlapping discs, but it works well also for practically arbitrary 2D domains. The method is based on a reformulation of the original differential boundary value problem into a system of integral equations, starting with the Poisson type integral formula for a disk. The derived system of integral equations can be solved by the standard Neumann-Ulam scheme, but it works only under some restrictions which are satisfied in the case of Laplace equation, and are not satisfied in the case of Lamé equation. To overcome this difficulty, we have constructed two different stochastic iterative procedures: (1) a Chebyshev-type iterations with random parameters, and (2) a SOR-based iteration procedure. The calculations have shown that the new SOR-based RWFS method considerably accelerates the convergence of the standard random Walk on Spheres method, and provides much higher accuracy, when applying to the Laplace equation. More interesting, the new SOR-based RWFS is the first convergent method with finite variance for solving the system of Lamé equations. Generally, there are no probabilistic representations for system of elliptic equations, and we believe that the idea behind our approach will give a rise to new attempts to construct such probabilistic solutions.

As mentioned above, the RWFS method is especially efficient for domains represented as a family of overlapping discs (or spheres, in 3D), but it works well also for domains which can be approximated by this kind of families. It should be noted that the standard Random Walk on Spheres (RWS) method where the last random sphere stops in an ε-boundary deals also with this type of domains. The difference in this sense is that in RWS, a huge number of random spheres is involved, while in RWFS, we approximate the domain by a family of deterministic spheres the number of which can be taken not large.

References

[1] Alturi S.N., Sladek J., Sladek V. Zhu T. The local boundary integral equation (LBIE) and it's meshless implementation for linear elasticity. *Computational Mechanics*, **25**, 180-198 (2000).

[2] Budaev B.V., Bogy D.B. Probabilistic approach to the Lame equations of linear elastostatics. International Journal of Solids and Structures, **40** (2003), N 23, 6285-6306.

[3] De S., Bathe K.J. The method of finite spheres. *Computational Mechanics*, **25**, 329-345 (2000).

[4] E.B. Dynkin. Markov Processes, Vol. I & II Springer-Verlag, Berlin, 1965.

[5] Elepov, B.S., Kronberg, A.A., Mikhailov, G.A. and Sabelfeld, K.K. *Solution of Boundary Value Problems by Monte Carlo Methods.* Nauka, Novosibirsk, 1980 (in Russian).

[6] Ermakov, S.M., Nekrutkin, W.W. and Sipin, A.S. *Random Processes for Classical Equations of Mathematical Physics.* vol. **34** of Math. Appl. (Soviet Series). Kluwer, Dodrecht, 1989.

[7] Gradstein, I.S. and Rygyk, I.M. *Tables of Integrals, Sums, Series and Products.* Nauka, Moscow, 1971 (in Russian).

[8] Hadjimos A., Plemmons R. Optimal p-cyclic SOR. *Numer. math.*, **67** (1994), 475-490.

[9] Kanevsky, V.A. and Lev, G.Sh. On simulation of the exit of a Wiener process from a ball. *Soviet J. on Numerical mathem. and mathem. physics* **17** (1977), No.3, 251-258.

[10] Ram P. Kanwal. Linear Integral Equations. Theory and Technique. Birkhaeser, Boston-Basel-Berlin. Second Edition, 1997.

[11] Klawon A., Pavarino L. Overlapping Schwarz methods for mixed linear elasticity and Stokes problems. *Computer methods Appl. Mech. Engrg.* **165**, 233-245 (1998).

[12] Kupradze, V.D., Gegelia, T.G., Basheleishvili, M.O. and Burkhuladze, T.V. Three Dimensional Problems of Mathematical Elasticity Theory. Nauka, Moscow, 1976 (in Russian).

[13] G.I. Marchuk and V.I. Lebedev. Numerical methods in the neutron transport theory. Atomizdat, Moscow, 1971 (in Russian).

[14] Mikhailov G.A. Minimization of computational costs of non-analogue Monte Carlo Methods. Series of Soviet and East European Mathematics, Vol. 5, World Scientific, Singapore, 1991.

[15] G.N. Milstein, M.V Tretyakov. Stochastic numerics for mathematical physics. Springer-Verlag. Berlin - Heidelberg - New York, 2004.

[16] P. Ossadnik. New model for crack growth using random walkers. HLRZ preprint 106/92.

[17] Roux, R. Generalized Brownian motion and elasticity. *J. Stat. Physics*, **48** (1987), 201–213.

[18] Niethanner W. The successive over relaxation method (SOR) and Markov chains. *Annals of Operations Research*, **103**, 351-358 (2001).

[19] Ripley B. Stochastic simulation. John Wiley & Sons, NY, 1987.

[20] Royster, W.C. A Poisson integral formula for the ellipse and some applications. *Proc. AMS.*, **15** (1964), 661-670.

[21] Sabelfeld, K.K. Vector Monte Carlo algorithms for solving systems of elliptic equations of the second order and the Lamé equation. *Dokl.Akad.Nauk SSSR*, **262** (1982), No.5, 1076–1080 (in Russian).

[22] Sabelfeld, K.K. *Monte Carlo Methods in Boundary Value Problems*. Springer-Verlag, Berlin – Heidelberg – New York, 1991.

[23] K. Sabelfeld. A method of random walks on fixed spheres for solving Neumann and mixed Neumann-Dirichlet boundary value problems. Proceedings of V IMACS Seminar on Monte Carlo methods. Tallahassee, USA, 2005, p.25-27.

[24] K.K.Sabelfeld and Ju.N.Kopylov. Applications of the walk on boundary algorithms. Preprint of Computing Center, N763, Novosibirsk, 1987 (in Russian).

[25] K.K. Sabelfeld, I.A. Shalimova, and A.I. Levykin. Discrete random walk over large spherical grids generated by spherical means for PDEs. *Monte Carlo Methods and Applications*, **10** (2004), N 3-4, 559–574.

[26] K.K. Sabelfeld, A.I. Levykin, and I.A. Shalimova. Random Walk on Fixed Spheres method for electro- and elastostatics problems. *Mathematics and Computers in Simulation*, 2006, in press.

[27] Sabelfeld, K.K. and Shalimova, I.A. *Spherical Means for PDEs.* VSP, The Netherlands, Utrecht, 1997.

[28] Sabelfeld, K.K. and Shalimova I.A. Random walk methods for static elasticity problems. *Monte Carlo Methods and Applications*, **8**, 2002, N2.

[29] Sabelfeld, K.K. and Simonov, N.A. *Random Walks on Boundary for Solving PDEs*. VSP, The Netherlands, Utrecht, 1994.

[30] Sobolev, S.L. The Schwarz algorithm in elasticity theory. *Doklady AN SSSR*, **4** (1936), 235–238 (in Russian).

[31] Vorobiev Ju.V. Stochastic iteration process. J. Comp. Math. and Math. Physics., vol.4 (1964), N6, 1088-1092, and vol. 5, N5, 787-795 (in Russian).

[32] Vorobiev Ju.V. Stochastic iteration process in the method of variable directions. J. Comp. Math. and Math. Physics., vol.8 (1968), N3, 663-670 (in Russian).

[33] D.M. Young. Iterative solution of large linear systems. Academic Press, New York and London, 1971.